Longitudinal analysis at three oral sites links oral microbiota to clinical outcomes in allogeneic hematopoietic stem-cell transplant

Vitor Heidrich[1,2], Franciele H. Knebel[1], Julia S. Bruno[1], Vinícius C. de Molla[3,4], Wanessa Miranda-Silva[1], Paula F. Asprino[1], Luciana Tucunduva[5], Vanderson Rocha[6], Yana Novis[5], Eduardo R. Fregnani[1], Celso Arrais-Rodrigues[3,4], Anamaria A. Camargo[1,*]

[1]Centro de Oncologia Molecular, Hospital Sírio-Libanês, São Paulo, SP, Brazil

[2]Departamento de Bioquímica, Instituto de Química, Universidade de São Paulo, São Paulo, SP, Brazil

[3]Hospital Nove de Julho, Rede DASA, São Paulo, SP, Brazil

[4]Universidade Federal de São Paulo, São Paulo, SP, Brazil

[5]Centro de Oncologia, Hospital Sírio-Libanês, São Paulo, SP, Brazil

[6]Hospital das Clínicas da Faculdade de Medicina, Universidade de São Paulo/Instituto do Câncer do Estado de São Paulo (ICESP), São Paulo, SP, Brazil

*Corresponding author

Authors' email addresses

VH: vheidrich@mochsl.org.br

FHK: fhknebel@mochsl.org.br

JSB: juliasb9@gmail.com

VCM: viniciuscamposdemolla@gmail.com

WMS: wmswanessa@yahoo.com.br

PFA: pasprino@mochsl.org.br

LT: luciana.tucunduva@gmail.com

VR: rocha.vanderson@hotmail.fr

YN: yananovis@yahoo.com

EFR: eduardofregnani@me.com

CAR: celsoarrais@gmail.com

AAC: anamaria.acamargo@hsl.org.br

Abstract

Background

Allogeneic hematopoietic stem-cell transplant (allo-HSCT) is a potentially curative therapy for several hematological disorders. Before stem-cell infusion, recipients undergo a conditioning regimen with chemo/radiotherapy and immunosuppressants, requiring the use of antibiotics to treat and prevent infections. This regimen promotes drastic alterations in the recipient's microbiotas, including the oral microbiota, which have been associated with allo-HSCT complications and poor outcomes. However, long-term longitudinal studies on the oral microbiota of allo-HSCT recipients are scarce and disregard the existence of distinct microbiotas within the oral cavity. Here, we used 16S rRNA gene sequencing to characterize the microbiota dynamics (during and after allo-HSCT) of 31 allo-HSCT recipients at 3 oral sites (gingival crevicular fluid, oral mucosa, and supragingival biofilm).

Results

Analysis of the oral microbiota dynamics during allo-HSCT revealed a significant decline in bacterial diversity and major shifts in microbiota composition in all oral sites, including blooms of potentially pathogenic genera. These blooms in some cases preceded respiratory infections caused by the blooming genera. We also noticed that differences in microbiota diversity and composition between oral sites were lost during allo-HSCT. Overall, oral microbiotas returned to their preconditioning state after engraftment. However, the ability to recover the initial bacterial composition varied between patients. After stratifying patients based on their ability to recover their preconditioning microbiota composition, we found that recovery of the oral mucosa microbiota composition was not associated with antibiotic usage but was associated with higher preconditioning diversity and earlier reconstitution of normal leukocyte counts. Most notably, oral mucosa microbiota composition recovery was an independent biomarker of better allo-HSCT outcomes.

Conclusion

We observed clear patterns of microbiota dysbiosis in all three oral sites during allo-HSCT, however each oral site responded differently to the perturbations associated with allo-HSCT. Oral microbiota injury and recovery patterns were associated with allo-HSCT complications and outcomes. This study highlights the potential clinical impact of the oral microbiota in the allo-HSCT setting and the clinical value of tracking oral microbiota changes during allo-HSCT.

Keywords

Oral microbiome; 16S rRNA gene sequencing; allogeneic hematopoietic cell transplant; microbiome stability; blooming of bacteria; biomarkers; clinical outcomes.

Introduction

Countless microbes from food, air, and our physical/biological environment arrive in our mouths daily. However, only a small subset of these microbes can colonize the oral cavity to compose the oral microbiota [1]. This constant contact with non-resident microbes and frequent exposure to other insults (e.g., toothbrushing) made the human oral microbiota remarkably stable and resilient to external perturbations [2].

Residing oral microbes organize in biofilms, creating oxygen gradients that allow colonization by both anaerobic and aerobic bacteria [1]. Differences in moisture, topography, and tissue type (shedding vs. non-shedding), among others, make each oral site home to distinct bacterial communities [1, 3] with main compositional differences existing between mucosa-associated and teeth-associated microbiotas [4].

These distinct oral microbiotas are important regulators of human health, as they have been associated with different local and systemic disorders [5]. While the supragingival biofilm is causally linked to the pathogenesis of dental caries [6], bacteria at the gingival crevice, an oxygen-limited environment bathed in immune exudate (gingival crevicular fluid), are linked to periodontitis [7] and may cause bacteremia by translocation to the circulation

79 across the thin gingival crevice epithelium [8]. Oral bacteria can further facilitate systemic
80 reach by producing molecules that increase vascular permeability [5]. Using this strategy,
81 oral *Porphyromonas gingivalis* is able to colonize the brain, contributing to the pathogenesis
82 of Alzheimer's disease [9].

83 Allogeneic hematopoietic stem-cell transplant (allo-HSCT) is used to treat malignant
84 (e.g., acute myeloid leukemia) and non-malignant (e.g., aplastic anemia) hematological
85 disorders [10]. The goal of allo-HSCT is to eradicate malignant/defective cells and to replace
86 an abnormal hematopoietic and immune system [11]. Allo-HSCT recipients undergo a
87 conditioning regimen with chemo/radiotherapy that reduces disease burden and provides
88 sufficient immunoablation to allow donor stem-cell engraftment [12]. After engraftment, the
89 graft-vs-tumor/autoimmunity effect further promotes disease eradication and the
90 hematopoietic/immune function gradually reconstitutes [13]. Besides chemo/radiotherapy,
91 allo-HSCT recipients are treated with immunosuppressants to prevent engraftment failure
92 and graft-vs-host disease, and antibiotics to prevent and treat opportunistic infections during
93 immunosuppression [13, 14].

94 Allo-HSCT is considered one of the most severe perturbations the immune system
95 undergoes in the therapeutic setting [15]. Since the immune system regulates microbiota
96 composition [16] and chemotherapy [17], radiotherapy [18], and antibiotics [19] have
97 detrimental effects on the microbiota, drastic alterations in the gut microbiota have been
98 reported in allo-HSCT recipients, including loss of bacterial diversity and blooms of
99 potentially pathogenic species [20]. Recent evidence shows these alterations extend to other
100 microbiotas [21], including the relatively more stable oral microbiota [22–26]. More
101 importantly, the pre-transplant microbiota and the extent of microbiota damage during allo-
102 HSCT are associated with allo-HSCT complications and outcomes, so that gut and oral
103 microbiota provide biomarkers in the allo-HSCT setting [24, 25, 27–30].

104 The stability of the oral microbiota [5] and its associations with allo-HSCT outcomes
105 offer a unique opportunity to identify predictive biomarkers and develop therapeutic
106 interventions to promote oral health in allo-HSCT recipients, potentially improving allo-HSCT

safety and efficacy. However, so far, oral microbiota studies in allo-HSCT recipients evaluated single oral sites, not leveraging the ease of sampling of different oral compartments [22–26, 30]. In addition, although a causal link between post-transplant gut microbiota recovery and improved clinical responses to allo-HSCT has been suggested [15], oral microbiota recovery trajectories after allo-HSCT were not thoroughly characterized and their association with allo-HSCT outcomes remain unknown.

To obtain a more in-depth understanding of oral microbiota dynamics during and after allo-HSCT and to test whether oral microbiota recovery is associated with allo-HSCT outcomes, we profiled the oral microbiota of a Brazilian cohort of allo-HSCT recipients. We collected over 440 samples encompassing five timepoints and three oral sites: gingival crevicular fluid (GCF), oral mucosa (OM), and supragingival biofilm (SB), which allowed a longitudinal anatomically-aware analysis of the oral microbiota. We used 16S rRNA gene sequencing to characterize diversity, compositional, and taxonomical changes in oral microbiota during allo-HSCT and after engraftment. We associated these changes with antibiotic usage and allo-HSCT complications. Finally, we evaluated recovery trajectories after allo-HSCT to associate oral microbiota recovery with allo-HSCT outcomes.

Materials and methods

Patients' clinical characteristics

Thirty-one patients undergoing allo-HSCT at Hospital Sírio-Libanês (São Paulo, Brazil) were recruited between January 2016 and April 2018. The median age was 50 years, most patients were male (55%), and acute leukemia was the most common underlying disease (58%; 11 acute myeloid leukemia and 7 acute lymphocytic leukemia cases). Most patients underwent reduced intensity conditioning (61%) and received grafts from peripheral blood (68%). Patient clinical information is summarized in Table S1.

5

Antibiotic usage analysis

Antibiotic prescriptions were retrieved retrospectively from clinical records. Information spanning 30 days before preconditioning sampling and 100 days after stem-cell infusion was collected to build timelines of antibiotic usage for each patient (Additional file 1: Timelines of antibiotic usage). A ridgeline plot of antibiotic usage detailing all antibiotics and antibiotic classes used showed antibiotics prescription concentrates in the few weeks immediately after infusion (Fig. S1), with only 5/31 patients receiving antibiotics before preconditioning (Additional file 1). Due to the sparse use of antibiotics before preconditioning and the unlikely effect of antibiotics received months after allo-HSCT on clinical outcomes, antibiotic usage was analyzed considering only the time window between preconditioning and 30 days after engraftment (a patient deceased during this period was excluded from the analysis). For each patient, the length in days under antibiotic therapy (length of therapy, LOT) and the number of agent days under antibiotic therapy (days of therapy, DOT) was calculated, as defined previously [31]. To evaluate the impact of specific antibiotic classes on microbiota dynamics, patients were further classified according to antibiotic class usage during the period of interest. Only antibiotic classes received by at least 20% of our patients (6/30) were considered in this analysis. In addition to individual antibiotics prescriptions, all patients underwent standard antimicrobial prophylaxis with antibiotic, antiviral and antifungal drugs. Because the standard antibiotic prophylaxis protocol in our institution comprises oral levofloxacin and sulfamethoxazole-trimethoprim, their use was not considered in the antibiotic usage analysis.

Sample collection

Patients were examined frequently by an oral medicine specialist throughout the hospitalization period. The standard oral hygiene protocol comprised toothbrushing with fluoridated toothpaste and 0.12% chlorhexidine mouthwash. Samples were collected at least six hours after the last oral hygiene procedure by an oral medicine specialist at three oral

sites. GCF samples were collected by inserting absorbent paper points in the gingival crevice; OM samples were collected by swabbing bilateral buccal mucosa, alveolar mucosa of the jaws, and tongue dorsum; SB samples were collected by swabbing all vestibular enamel surface. Samples were dry-stored at -20ºC.

DNA extraction and 16S rRNA gene amplicon sequencing

Samples were brought to room temperature. Bacterial cells were recovered from swabs or paper points by vortexing in 600 µl or 800 µl TE buffer (10mM Tris; 1mM EDTA; pH 8,0), respectively. Samples were transferred to a new tube, supplemented with 6 µl (OM and SB) or 8 µl (GCF) PureLink™ RNAse A (20 mg/ml; Invitrogen), and DNA was extracted using the QIAamp DNA Mini Blood kit (Qiagen) following the manufacturer's protocol (*Buccal Swab Spin Protocol*).

Bacterial communities were profiled by 16S rRNA gene amplicon-sequencing as described in detail previously [32]. In short, amplicon libraries were prepared with 12.5 ng of total DNA and pre-validated V3V4 primers [33] following Illumina's protocol (*Preparing 16S Ribosomal RNA Gene Amplicons for the Illumina MiSeq System*). Amplicons were sequenced on the Illumina MiSeq platform using the MiSeq Reagent Kit v3 (600-cycle) (Illumina).

Bioinformatics pipeline

Reads were demultiplexed using the MiSeq Reporter Software. Primers were removed and low-quality 3' ends were trimmed using *seqtk* [34]. Next, reads were processed using QIIME 2 (v2019.10.0) as schematized in Fig. S2a [35]. In detail, amplicon sequence variants (ASVs) were generated using the DADA2 pipeline (via *q2-dada2*), which includes removal of low-quality reads, denoising, merging, and removal of bimeras [36]. Chimeric ASVs were further filtered out using a reference-based approach with VSEARCH [37] (via *q2-vsearch*) and SILVA database (v132) [38]. Taxonomic assignment of ASVs was also performed with VSEARCH [37] (via *q2-feature-classifier*) and SILVA (v132) [38]. Finally,

7

non-bacterial ASVs were removed (via *q2-feature-table*). QIIME 2 outputs were transferred to the R environment [39] using the *qiime2R* R package [40] and analyzed for microbiota profiling with custom R scripts as detailed below.

Microbiota and statistical analyses

The total number of reads of the sample with the lowest number of reads (3,578 reads) among the samples included in the microbiota profiling analyses was used as C_{min} for Scaling with Ranked Subsampling (SRS) normalization prior to diversity analyses [41]. Diversity was measured by the Gini-Simpson index [42] using the *phyloseq* R package [43]. Longitudinal diversity variations were evaluated by calculating diversity resistance, resilience, and stability [44, 45] (see Additional file 3: Supplementary methods). Compositional dissimilarity between samples was measured by the weighted UniFrac distance [46] using the *rbiom* R package [47]. Longitudinal compositional variations were evaluated by calculating compositional stability (see Additional file 3). Multiple linear regression was used to evaluate whether antibiotic usage was associated with diversity stability and compositional stability (see Additional file 3). Recovery to baseline composition was defined as distance between samples collected at preconditioning and 30 days after engraftment <0.5.

Taxonomic nomenclature was homogenized prior to all taxonomic analyses (see Additional file 3). Taxa relative abundance plots included only the most relevant genera according to criteria specified in figure legends. Differential abundance analysis was performed using ANCOM-BC [48] with genera present in ≥25% of the samples being compared. Genera abundance differences between groups at q-value < 0.05 (Bonferroni correction) were considered statistically significant, including ANCOM-BC structural zeroes.

Associations between oral microbiota composition recovery or clinical parameters with allo-HSCT outcomes were determined using univariate Cox proportional-hazards regression [49] or univariate Fine-Gray competing risk regression [50]. Cox models were used to evaluate overall survival and progression-free survival, while Fine-Gray models were

used to evaluate the risk of transplant-related death (with relapse mortality as competing risk) and the risk of underlying disease relapse (with transplant-related mortality as competing risk). Multivariate analysis was used to evaluate oral microbiota composition recovery and correct for clinical parameters significantly associated with the outcome (P-value < 0.05) in the univariate analysis. Patients experiencing the event before oral microbiota composition recovery evaluation were excluded from univariate and multivariate analyses.

Results

Samples collected and sequencing output

We collected samples from three oral sites (GCF, OM, and SB) at five timepoints during allo-HSCT: preconditioning (P), aplasia (A), engraftment (E), 30 days after engraftment (E30), and 75 days after engraftment (E75). Since most patients were discharged shortly after engraftment, the exact date of sample collection varied for E30 (20–45 days after engraftment) and E75 (60–131 days after engraftment) samples, as indicated in Fig. S3. Premature death after allo-HSCT hampered the collection of the E30 sample for patient #3 and E75 samples for patients #1, #2, #3, #21, and #31 (Fig. S3). In addition, the E75 sample from patient #9 was excluded due to low DNA yield. Overall, 444 samples were successfully processed and sequenced for microbiota profiling.

We generated a total of 53,253,725 V3V4 16S rRNA reads (median per sample: 104,230.5; range: 2,059–502,409; Fig. S2b). After filtering, 31,343,619 reads (59%; Fig. S2c–d) were retained (median per sample: 63,075.5; range: 87–310,082; Fig. S2e), corresponding to 4,046 ASVs. Using SRS curves [51] (Fig. S4), we established a minimum sequencing depth cutoff of 3,000 reads and 4 low-depth samples were excluded from further analysis (patient #1, OM, P; #5, OM, E; #6, OM, E; #25, SB, E). We proceeded to profile the oral microbiota during allo-HSCT with 440 samples.

9

Compositional differences between oral microbiotas during allo-HSCT and after engraftment

We first assessed microbiota compositional differences between oral sites at each allo-HSCT timepoint. Visually, all three oral microbiotas occupied a similar compositional space throughout allo-HSCT (Fig. 1a). Nevertheless, similarly to what is observed in healthy adults [4], each oral site contained a significantly different microbiota composition at P (PERMANOVA, GCF vs. OM: P-value = 0.001; GCF vs. SB: P-value = 0.002; OM vs. SB: P-value = 0.018). Noteworthy, these differences progressively diminished in subsequent timepoints until E30 and were partially recovered at E75 (Fig. 1b). Calculation of the minimum compositional distance between oral sites for each patient confirmed lower compositional distance between sites after P (Fig. 1c).

Differential abundance analysis at genus level using ANCOM-BC revealed a similar picture (Fig. 1d). As expected, all three oral microbiotas showed many distinguishing genera at P. For example, we observed a higher abundance of *Actinomyces* in the SB as compared to GCF and a higher abundance of *Solobacterium* in the OM as compared to SB (Fig. S5). *Actinomyces spp.* are early colonizers of the SB with a crucial role in ecological succession during SB maturation [52]. On the other hand, *Solobacterium moorei*, the only known species in the *Solobacterium* genus, is a halitosis-associated bacteria typically found in the tongue dorsum [53], a site contemplated in OM samples. However, a smaller number of differentially abundant genera was observed in subsequent timepoints, with a slight increase in the number of differentially abundant genera between sites at E75, illustrated by the reappearance of *Solobacterium* as an OM-associated genus (Fig. S5).

In short, our data indicate that compositional differences between oral microbiotas are reduced during allo-HSCT, being only partially recovered several weeks after engraftment.

Oral microbiota dynamics during allo-HSCT and after engraftment

We next characterized microbiota diversity dynamics at each oral site during allo-HSCT and after engraftment. As previously shown for OM [25] and SB [24], GCF presented a stepped decline in diversity up to E (Fig. 2a). By extending this analysis to the post-engraftment period for all oral sites, we observed a gradual recovery of diversity, with baseline levels almost fully reestablished around E75.

We then applied key concepts from ecology [45] for a more in-depth characterization of diversity dynamics during allo-HSCT. By considering allo-HSCT as a perturbation relieved immediately after engraftment, we calculated for each patient diversity resistance (inversely proportional to the diversity loss up to E), resilience (rate of diversity gain after E), and stability (combined effect of resistance and resilience) to allo-HSCT (Fig. S6a; see Additional File 3). GCF showed higher diversity resistance than OM and SB (Fig. 2b), in line with the less pronounced loss of diversity observed in this oral site at E (Fig. S6b). All oral sites presented equivalent levels of diversity resilience and stability (Fig. 2b), in line with the similar levels of diversity after engraftment observed for all oral sites (Fig. S6b).

Next, we characterized compositional changes in each oral site during allo-HSCT and after engraftment. The compositional distance to P centroid increased up to E and decreased in the post-engraftment period, indicating a displacement from and posterior recovery to baseline compositions (Fig. 1c). However, when comparing the compositional distance from P to all other timepoints using PERMANOVA tests, we observed that GCF and SB post-engraftment samples still showed significantly different compositions after engraftment compared to P, while OM samples more fully recovered their preconditioning state (Fig. 1d). Finally, in analogy to diversity stability, we calculated the compositional stability for each patient (see Additional File 3). As observed for diversity stability, all oral sites showed equivalent levels of compositional stability (Fig. S6c).

11

Our data indicate that allo-HSCT transiently damages oral microbiotas diversity and composition, but each oral site responds differently to the perturbations associated with allo-HSCT.

Oral taxa abundances during allo-HSCT and after engraftment

The loss of differences between microbiotas of distinct oral sites and the displacement from initial compositions observed during allo-HSCT point out to a complex compositional dynamics that likely involves many bacterial taxa and thus can be better appreciated by longitudinal taxonomic composition analysis at each specific site. As expected, all oral sites presented high relative abundance of commensal bacteria at P (Fig. 3a; Fig. S7). For instance, *Veillonella* and *Streptococcus*, genera with high relative abundance in all oral sites of healthy adults [4], occupied either the first or second position in terms of mean relative abundance at P in all three oral sites (Fig. 3b). However, there were several changes in the ranking of the most abundant taxa (on average) across timepoints (Fig. 3b; Fig. S7), pointing to drastic taxonomic composition changes during allo-HSCT. There are some noteworthy examples, such as *Streptococcus* in SB, which went from first in the relative abundance ranking at P to the eleventh position at E. Interestingly, *Streptococcus* recovered its initial ranking position after engraftment (first position at E30 and E75). On the other hand, some non-commensals genera were close to absent in P and only emerged in the subsequent timepoints. For instance, *Enterococcus* and *Lactobacillus*, both potentially pathogenic genera in the oral microbiota [54, 55], showed low mean relative abundance at P but were among the most abundant genera in all sites at E.

Differential abundance analysis at genus level using ANCOM-BC with P as reference for comparisons confirmed these results and showed several additional differentially abundant genera (Fig. 3c). The number of differentially abundant genera at each timepoint was consistent with the compositional displacement and recovery aforementioned, with a maximum of differentially abundant genera at E (Fig. S8). Although there were considerably fewer differentially abundant genera after engraftment, some differences persisted. For

instance, we observed a decreased abundance of *Catonella* in OM and SB, and of Tannerella in GCF at E75, suggesting a long-lasting reduction of these genera caused by allo-HSCT.

In summary, we observed that the dynamics of some commensal bacteria reproduce the same pattern of displacement during allo-HSCT and recovery after engraftment observed for the overall community. We also observed the emergence of opportunistic potentially pathogenic genera during the most perturbed allo-HSCT phase which are capable of colonizing all three oral sites and likely contribute to the loss of compositional differences between oral microbiotas observed after preconditioning.

Emergence of opportunistic genera and allo-HSCT complications

The emergence of opportunistic genera during allo-HSCT can be more rigorously quantified by assessing taxa blooms, defined as a taxon relative abundance increase from <1% at P to dominance levels (≥30%) at any subsequent timepoint. We have previously shown, by analyzing this same cohort, blooms of specific genera occurring in SB during A and E [24]. We now extended this analysis to other oral sites and to the post-engraftment period. Overall, we detected 81 blooms, involving 22 genera and 27/31 patients. All oral sites showed several blooming events, but SB blooms were more frequent (SB: n = 35; GCF: n = 24; OM: n = 22; Fig. 4a) and significantly more prevalent (SB: 23/31; GCF: 14/31; MO: 16/30; chi-square test, P-value = 0.022). Blooms typically occurred at E (53% of events; Fig. 4b) and were rapidly resolved in the post-engraftment period.

Lactobacillus (15%), *Enterococcus* (12%), and *Staphylococcus* (10%) were the genera most frequently observed in blooming events in the oral microbiota during allo-HSCT (Fig. 4c). But oral sites differed in the genera typically associated with blooms (Fig. 4d). SB showed mainly *Enterococcus* (7 events) or *Lactobacillus* (6) blooms, while GCF showed mostly *Staphylococcus* (4) or *Lactobacillus* (4) blooms. In contrast, OM blooms showed a less clear signal of blooming genera. Nevertheless, some patients presented concomitant blooms of the same genus in all oral sites.

We noticed that many of the blooming genera are potentially pathogenic for allo-HSCT recipients. For instance, *Staphylococcus* genus contains species related to several infections, including hospital-acquired pneumonia [56], an allo-HSCT complication with 15-30% incidence [57]. Therefore, we evaluated whether blooming events in the oral microbiota were associated with respiratory infections in our cohort. Between P and E75, only 3/31 patients presented bacterial respiratory infections (patients #1, #2, and #7). All three patients showed blooms of genera in the oral microbiota during allo-HSCT. Specifically, patient #1 presented blooms of *Enterococcus* (in GCF and SB at E) and Acetobacter (in GCF and SB at E30), patient #2 presented blooms of *Stenotrophomonas* (in all oral sites at E) and *Mycoplasma* (in GCF at E), and patient #7 presented blooms of *Mycoplasma* (in OM and SB at E). Interestingly, patients #1 and #2 presented blooms of the same genus identified in the microbiological exam of their respiratory tract samples: *Enterococcus* and *Stenotrophomonas*, respectively. Importantly, these blooms preceded the clinical manifestation of the respiratory infection by one and two weeks, respectively, suggesting a potential oral origin for the bacteria associated with the respiratory infections in these cases. On the other hand, patient #7 developed a respiratory infection caused by *Escherichia coli* between E30 and E75, which was unrelated to the blooms detected for this patient.

Given the apparent translocation of abundant oral bacteria to the respiratory tract in our cohort and the well-known association between intestinal dominance and bacteremia during allo-HSCT [58], we also tested whether blooming events in the oral microbiota were associated with bacteremia events. Positive blood cultures for bacteria were detected for 15/31 patients between P and E75. We did not find an association between oral microbiota blooms and altered odds of bacteremia (Fisher's exact test, GCF bloom: OR = 3.17, P-value = 0.156; OM bloom: OR = 2.25, P-value = 0.299; SB bloom: OR = 0.92, P-value = 1; any site bloom: OR = 3.12, P-value = 0.600). We detected a single case in which the blooming of a genus in the oral microbiota preceded a bacteremia event with the same genus involved. In detail, patient #14 presented blooms of *Enterococcus* in GCF and SB at A, which preceded positive blood cultures for *Enterococcus* by 1.5 weeks.

Overall, we observed that blooms of opportunistic genera occur frequently in oral microbiota during allo-HSCT, especially in SB. The examples described suggest oral microbiota blooms during allo-HSCT may trigger translocation of oral microbes to the respiratory tract (as often happens during oral microbiome dysbiosis [56]) and cause respiratory infections in allo-HSCT recipients.

Impact of antibiotic usage on oral microbiota dynamics

To investigate the impact of antibiotic usage on oral microbiota dynamics and blooming events during allo-HSCT, we analyzed antibiotic usage data between P and E30 (see Materials and Methods). Antibiotic usage varied widely across patients in terms of length of therapy (LOT range: 0–58 days; median: 15.5 days) and days of therapy (DOT range: 0–112 days; median: 22 days) (Table S1). Overall, 17 antibiotic agents (range: 0-10; median: 3), spanning 12 distinct antibiotic classes (range: 0–9; median: 3 antibiotics) were administered to our patients. The antibiotics administered to each patient are illustrated in Fig. 5a. Most patients received cefepime (73%) and meropenem (63%), making cephalosporins and carbapenems the most frequently used antibiotic classes: 73% and 63%, respectively (Fig. S9a). Glycopeptides and penicillins were also used in a considerable proportion of patients: 60% and 23%, respectively. All other antibiotic classes were used by less than 17% of our patients (Fig. S9b).

First, to assess the effect of antibiotic usage in microbiota dynamics, we modeled diversity stability (which incorporates diversity resistance and resilience) and compositional stability using antibiotic usage information (Table S2). We found that DOT significantly predicted diversity stability during allo-HSCT for all oral sites, with prolonged use of antibiotic therapy associated with lower diversity stability. However, the use of specific antibiotic classes was not associated with altered diversity stability (Table S2). On the other hand, DOT was not a predictor of compositional stability, but glycopeptide usage was significantly associated with decreased SB compositional stability (Table S2). In addition, we found non-significant associations at P-value < 0.1 between other antibiotic classes and decreased

15

compositional stability in GCF (cephalosporins and penicillins) and SB (cephalosporins), while OM compositional stability was clearly less impacted by antibiotic usage during allo-HSCT (Table S2).

We next tested whether blooms at different oral sites were associated with antibiotic usage. E75 blooms were not considered in this analysis since our antibiotic usage survey focused on the period between P and E30 (see Materials and Methods). With one exception (glycopeptides and GCF blooms), the use of specific antibiotic classes was not associated with blooms, but patients experiencing blooms showed higher LOT and DOT (Fig. 5b), although it is not clear whether a more extended period under antibiotic therapy was the cause or consequence of the blooms.

GCF blooms were significantly associated not only with LOT and DOT but also with the use of glycopeptides (Fisher's exact test, odds ratio (OR) = 15.65, P-value = 0.006, P-adjusted = 0.025), which enabled the investigation of the relation between the timing of glycopeptide usage and GCF blooming events. GCF blooms occurred in 12 patients up to E30, out of which 11 used glycopeptides (vancomycin and/or teicoplanin) between P and E30. Notably, 10/11 patients that used glycopeptides and experienced GCF blooms received glycopeptides a few days before or during the interval in which the bloom was detected, indicating that glycopeptide usage during allo-HSCT may cause blooms of genera in the oral microbiota.

The relationship between glycopeptide usage and blooming events and its consequences can be illustrated by the genera composition trajectories and antibiotic usage timeline of patients #1 and #2. Patient #2 experienced *Stenotrophomonas* blooms in all sites at E, which occurred during the administration of vancomycin (Fig. 5c). Two weeks after these blooms, patient #2 developed a respiratory infection caused by *Stenotrophomonas maltophilia*, detected in microbiological exams of respiratory tract samples (e.g., bronchoalveolar lavage). Despite the intensification in the use of antibiotics, *Stenotrophomonas* levels only rose in the oral microbiota after E, reaching staggering levels at E30 (>95% relative abundance in all oral sites). Analysis at ASV level revealed that

Stenotrophomonas ASVs were absent in patient #2 at P (relative abundance = 0% in all oral sites). At A, during the first course of vancomycin (Fig. 5c), a *Stenotrophomonas maltophilia* ASV emerged in the SB (relative abundance = 0.02%). This ASV would later be responsible for the blooms at E and the domination observed at E30. Taken together, these results suggest that the use of vancomycin during allo-HSCT allowed the emergence and the bloom of pathogenic *Stenotrophomonas maltophilia* in oral microbiota, which later translocated to the respiratory tract, causing a respiratory infection. Patient #1 presented a similar picture (Fig. S10), with the use of vancomycin followed by *Enterococcus* blooms and a subsequent respiratory infection caused by *Enterococcus faecium*. Notably, patients #1 and #2 died before E75, with death causes at least partially associated with their respiratory infections.

In summary, greater time of antibiotic exposure was associated with lower microbiota diversity stability and blooms in all oral sites. Glycopeptide usage was associated with lower microbiota compositional stability in SB and, although direct evidence is lacking, it seems causally linked to some of the blooming events.

Inter-patient variability in oral microbiota dynamics during allo-HSCT and after engraftment

To investigate inter-patient variability in oral microbiota dynamics during allo-HSCT and after engraftment, we assessed longitudinal changes in oral microbiota in a patient-centered analysis. Although most patients presented high diversity stability, which was achieved either by having high resistance, high resilience, or a balance between the two, some patients presented low diversity stability and even negative resilience values (Fig. 6a), indicating loss of diversity after E. Curiously, this inter-patient variability was not due to different levels of baseline diversity, since diversity at P was not correlated with diversity resistance, resilience, nor stability (Fig. S11a). Compositional stability was also not correlated with diversity levels at P (Fig. S11b)

In addition, when representing samples from all timepoints using Principal Coordinate Analysis (PCoA), we noticed that confidence intervals for E samples were larger, indicating

considerable inter-patient compositional variability under perturbation (Fig. S11c). To confirm this observation, we determined the most perturbed timepoint by quantifying the extent of compositional shifts between timepoints. As presented in Fig. 6b, compositional changes were more pronounced between A and E. Next, we evaluated inter-patient compositional variability at each timepoint either by assessing the compositional distance between samples and the respective timepoint centroid (Fig. 6c) or by calculating for each timepoint all pairwise compositional distances (Fig. 6d). Both results confirmed maximum inter-patient compositional variability at E under maximized perturbation, underscoring that allo-HSCT modifies oral microbiota differently for each patient.

Finally, we investigated if this variability in oral microbiota dynamics during allo-HSCT influenced oral microbiota recovery after engraftment. Although our results indicate that post-engraftment samples overall occupy a similar compositional space in comparison to P, this does not necessarily imply that patients recover their respective initial oral microbiota compositions after engraftment. In order to evaluate oral microbiota compositional recovery per patient, we analyzed the compositional distance from P for each patient and each site during allo-HSCT and after engraftment. Interestingly, we noted that even though most patients showed a recovery trajectory after engraftment, some did not (Fig. 6e).

Our data indicate a marked inter-patient variability in oral microbiota dynamics in response to allo-HSCT. Despite oral microbiotas as a whole resembling preconditioning microbiotas after allo-HSCT, patients differ in their ability to recover their initial oral microbiota composition.

Recovery of oral microbiota composition and allo-HSCT outcomes

To investigate whether oral microbiota recovery after allo-HSCT was associated with allo-HSCT outcomes we grouped our patients based on their ability to recover their preconditioning composition. We calculated the compositional distance between P and E30, and classified patients as recoverers (distance <0.5) or non-recoverers (distance ≥0.5). We further illustrate these contrasting recovery behaviors using PCoA with compositional

trajectories of a representative OM recoverer and of an OM non-recoverer (Fig. 7a). PCoAs for each patient are presented in Fig. S12. Overall, 77, 69, and 77% of our patients recovered their initial GCF, OM, and SB microbiota composition after engraftment, respectively (Fig. 7b).

Next, we used univariate analysis to investigate whether oral microbiota recovery after allo-HSCT was associated with allo-HSCT outcomes (Table S3; Fig. S13). Interestingly, OM recovery was associated with prolonged overall survival (OS; hazard ratio (HR) [95% confidence interval (CI)] = 0.17 [0.05–0.52], P-value = 0.002; Fig. 7c), prolonged progression-free survival (PFS; HR [95% CI] = 0.06 [0.01–0.34], P-value = 0.001; Fig. 7d), and a lower risk of underlying disease relapse (HR [95% CI] = 0.20 [0.06–0.69], P-value = 0.011; Fig. 7e). OM recovery, however, was not associated with altered risk of transplant-related death and GCF recovery or SB recovery were not associated with allo-HSCT outcomes (Table S3; Fig. S13).

To identify possible confounding variables, we used univariate analysis to investigate whether clinical parameters (including antibiotic usage; Table S1) were associated with allo-HSCT outcomes (Table S4–7). We found that disease risk index (DRI), conditioning intensity, and DOT were significantly associated with OS (Table S4). DRI was also associated with PFS (Table S5) and the risk of underlying disease relapse (Table S6). We then used a multivariate analysis to assess whether OM recovery was an independent predictor of allo-HSCT outcomes (Table S8). In all cases, OM recovery remained significantly associated with prolonged OS (HR [95% CI] = 0.09 [0.02–0.35], P-value < 0.001; Fig. 7f), prolonged PFS (HR [95% CI] = 0.09 (0.02–0.49), P-value = 0.005; Fig. 7g), and with a lower risk of underlying disease relapse (HR [95% CI] = 0.19 [0.06–0.55], P-value = 0.003; Fig. 7h). Taken together, these results robustly indicate that OM recovery at E30 is an independent biomarker of better allo-HSCT outcomes.

Underlying factors associated with oral mucosa microbiota recovery

Given the relevant associations between OM recovery and allo-HSCT outcomes, we searched for underlying factors associated with OM recovery. OM recovery was not associated with clinical parameters such as age, underlying disease, and graft source (Table S9). The usage of specific antibiotic classes, LOT, and DOT between P and E30 were also not associated with OM recovery (Table S9; Fig. S14a). In addition, OM recoverers and non-recoverers showed similar intervals between stem-cell infusion and engraftment (Fig. S14b).

We also evaluated whether OM microbiota characteristics could be related to OM recovery. OM recoverers did not show higher OM diversity at E30 (Fig. 8a), indicating OM non-recoverers did not necessarily possess dysbiotic OM microbiotas at E30. In line with this, OM blooms throughout allo-HSCT were not more frequent among OM non-recoverers (Fisher's exact test, OR = 4.07, P-value = 0.13). On the other hand, OM recoverers showed higher OM diversity at P and E (Fig. 8a). In fact, there was a significant negative correlation between OM diversity at P and the compositional distance between P and E30 (Fig. 8b). This effect was not observed for GCF and SB (Fig. 8b).

Lastly, we investigated if earlier reconstitution of blood cell counts was associated with OM recovery (see Additional File 3; Fig. 8c). Blood cell counts at P or E were not associated with OM recovery. Interestingly, however, OM recoverers showed higher leukocyte counts at E30, which is mostly due to significantly higher neutrophil and lymphocyte counts in this group. Furthermore, normal (within reference values) leukocyte counts at E30 were more frequently observed among OM recoverers compared to OM non-recoverers (16/20 vs. 3/9, respectively; Fisher's exact test, P-value = 0.032) and OM recoverers presented higher leukocyte counts throughout one year after allo-HSCT compared to non-recoverers due to the combined contribution of higher neutrophil, lymphocyte, and monocyte counts (Fig. S14c).

In summary, we found independent (blood cell counts) and non-independent (OM microbiota at P) parameters to illuminate the differences between OM recoverers and non-

20

recoverers. OM recovery was associated with higher diversity at P, indicating more diverse OM communities are more competent in recovering their pre-perturbation compositions. In addition, OM recoverers showed higher leukocyte counts at E30, suggesting an association between OM microbiota composition recovery and earlier immune system reconstitution.

Discussion

The anatomical complexity of the oral cavity provides a multitude of physicochemical environments for microbes to thrive [1, 3]. Although several dozen core bacterial genera inhabit all oral compartments, different species occupy each oral niche, meaning oral microbes are site-specialists that compose distinct microbiotas in each oral environment [1, 59]. We and others have previously reported the impact of allo-HSCT in oral microbiotas and their associations with allo-HSCT complications and outcomes [22–26, 30]. However, these studies analyzed single oral sites and were mostly limited to the peri-engraftment period of allo-HSCT. To our knowledge, this is the first study to evaluate the impact of allo-HSCT in the microbiota of various oral sites simultaneously during and after allo-HSCT.

We found that the microbiota of all oral sites was severely damaged by allo-HSCT, but each site responded differently to the perturbations associated with allo-HSCT. Compositional differences between oral sites were lost during allo-HSCT and partially recovered after engraftment. Oral microbiota injury was marked by loss of diversity and emergence of opportunistic potentially pathogenic genera. Notably, these opportunistic genera could colonize all three oral sites and likely contributed to the loss of compositional differences between oral microbiotas observed after conditioning. Colonization by opportunistic genera was more common at E, explaining the higher compositional variability and lower diversity observed at E, which we found to be the most perturbed allo-HSCT phase for all oral sites. This is in line with the Anna Karenina Principle applied to host-associated microbiomes [60], which states that more diverse communities tend to be more

21

553 compositionally similar, while perturbed communities tend to occupy several alternative
554 dysbiotic states.

555 Blooms of opportunistic genera were associated with prolonged antibiotic exposure
556 and the use of glycopeptides. This association is clinically relevant in the allo-HSCT setting
557 since glycopeptide-resistant bacteria (e.g., vancomycin-resistant enterococci) are a common
558 cause of infections in the hospital environment [61], especially in immunosuppressed
559 individuals. In addition, we observed that, in some cases, oral microbiota blooms preceded
560 respiratory infections caused by the blooming bacteria, linking the oral microbiota dynamics
561 during allo-HSCT to a common allo-HSCT complication [62], probably due to translocation of
562 oral bacteria to the respiratory tract through aspiration [56]. Similarly to our study, Thänert et
563 al. (2019) showed pathobiont blooms in the gut microbiota often preceded urinary tract
564 infections, but, as observed here, not all blooms were associated with subsequent infection
565 [63]. Interestingly, even though the mouth is a highly vascularized organ and the existence of
566 an oral-blood translocation axis has been proposed [64], we did not find a clear association
567 between oral bacteria blooms and bacteremia events during allo-HSCT.

568 Respiratory infections following blooms were caused by *E. faecium* in patient #1 and
569 *S. maltophilia* in patient #2. *S. maltophilia* colonization has been reported in 7% of allo-HSCT
570 recipients and is associated with higher non-relapse mortality risk due to higher odds of
571 invasive *S. maltophilia* infections [65]. Our results highlight that nosocomial bacteria such as
572 *S. maltophilia* can colonize the oral cavity during allo-HSCT. These results point to the
573 importance of maintaining oral health during allo-HSCT not only to prevent oral but also
574 distal complications (e.g., hospital-acquired pneumonia) [56]. Furthermore, our results
575 suggest that tracking drastic oral microbiota changes during allo-HSCT may guide early
576 interventions to prevent infections. This will be especially useful when the causative agent is
577 not a common respiratory pathogen such as in the case of *E. faecium* [66].

578 Longitudinal analysis of oral microbiota diversity and composition showed post-
579 transplant oral microbiotas were overall similar to preconditioning microbiotas, but patient-
580 level analysis showed that 23-31% of the patients did not recover their preconditioning

581 microbiota composition. Variability in gut microbiota recovery following a perturbation has
582 been previously described [67, 68], including after allo-HSCT, where most patients (>90%)
583 were unable to recover their initial gut microbiota composition [68]. The higher proportion of
584 patients that recovered their preconditioning composition in our study suggests that the oral
585 microbiota is more resilient to the perturbations associated with allo-HSCT than the gut
586 microbiota. This result is in line with a previous study showing that the oral microbiota is
587 more resilient than the gut microbiota to antibiotic perturbation [69].

588 Pre-perturbation microbiota characteristics, such as the presence of keystone
589 bacteria, influence microbiota recovery [70]. Here, we found that patients that recovered their
590 OM microbiota composition after allo-HSCT showed higher preconditioning OM diversity,
591 indicating that more diverse OM microbiotas are more resilient to allo-HSCT. Our results
592 converge on the insurance hypothesis, which proposes that high-diversity communities are
593 less susceptible to perturbations [71]. Interestingly, in our study, OM compositional recovery
594 was not associated with the use of specific antibiotics nor with the duration of antibiotic
595 exposure. This is possibly because OM microbiota composition is not impacted by
596 antibiotics, as evidenced by the lack of associations between antibiotic usage and OM
597 compositional stability. Host genetics, reestablishment of normal diet, and reconstitution of
598 the immune system are other possible drivers of microbiota recovery after allo-HSCT. Here,
599 we showed that leukocyte blood counts at E30 were higher in patients that recovered their
600 OM microbiota composition, indicating a close link between early immune system
601 reconstitution and oral microbiota recovery. We can speculate that immune reconstitution
602 allows stricter control of microbiota compositions (e.g., via immunoglobulin A [72]), which,
603 along with reestablishment of microbial environment (e.g., normal diet), supports the
604 recovery of the initial OM microbiota composition [73, 74].

605 The ability to recover the OM initial microbiota composition was associated with
606 better allo-HSCT outcomes. However, it is unclear if OM microbiota recovery is just a
607 consequence or also a driver of early immune reconstitution, thus having a causal role in the
608 improved outcomes following allo-HSCT. Evidence from gut microbiota studies indicates that

609 the latter hypothesis is plausible [75]. For instance, recent studies have shown that specific
610 gut microbes are associated with immune cell dynamics post-allo-HSCT [15, 76]. Similarly,
611 Miltiadous et al. (2022) found that higher peri-engraftment gut microbiota diversity was
612 associated with higher lymphocyte counts 100 days after transplant [77]. In addition, murine
613 model experiments showed that gut microbiota supports immune reconstitution by allowing a
614 higher dietary energy uptake [78]. Most importantly, in a controlled randomized clinical trial,
615 patients who received autologous fecal microbiota transplant after allo-HSCT showed higher
616 leukocyte counts 100 days after engraftment, indicating recovery of the gut microbiota has a
617 causal role in facilitating immune system reconstitution [15]. If this causal relationship
618 extends to the oral microbiota, the use of therapeutic interventions to promote oral health
619 and microbiota recovery in allo-HSCT recipients, such as oral microbiota transplants [79],
620 could potentially improve allo-HSCT outcomes.

621 An important limitation of our study is its small sample size, which did not allow
622 underlying disease stratification to parse the effect of different diseases on oral microbiota
623 dynamics. Still, the longitudinal design, assessment of different oral sites, and evaluation of
624 a Brazilian cohort (a population underrepresented in human microbiome studies [80]) with
625 extensive metadata publicly available are strengths of our study that should be highlighted.
626 Also, to better address the influence of oral bacteria in immune cell dynamics, future studies
627 will have to combine high temporal resolution oral microbiota data with more deeply
628 phenotyped immune cell counts (e.g., flow cytometry data). In addition, since 16S rRNA
629 amplicon sequencing has limited taxonomic resolution, further studies should ideally be
630 performed using shotgun metagenomic sequencing, as this would allow strain-level
631 dynamics tracking. Finally, here and previously [24, 25], we showed that associations
632 between gut microbiota and allo-HSCT outcomes broadly extend to the oral microbiota.
633 However, studies with synchronous gut and oral microbiota profiling will be necessary to
634 decipher how these microbiotas are linked during allo-HSCT, especially considering the
635 higher translocation of oral bacteria along the oral-gut axis during disease [81].

Conclusions

The oral cavity is the ultimate doorway for microbes entering the human body. We analyzed oral microbiotas dynamics in allo-HSCT recipients and showed that microbiota injury and recovery patterns were highly informative on allo-HSCT complications and outcomes. Our results highlight the importance of tracking recipient's microbiotas changes during allo-HSCT to improve our understanding of allo-HSCT biology, safety, and efficacy.

Availability of data and materials

The bioinformatics pipeline used to process the sequencing data, the R scripts used to run the analyses and generate the figures, and all clinical metadata (anonymized) necessary to reproduce these results are available at https://github.com/vitorheidrich/oral-microbiota-hsct. Raw sequencing data have been deposited in the European Nucleotide Archive (ENA) at EMBL-EBI under accession number PRJEB53914. Some samples (analyzed in past studies) were deposited previously in ENA at EMBL-EBI under accession numbers: PRJEB42862, PRJEB49175.

Abbreviations

A: Aplasia

Allo-HSCT: Allogeneic hematopoietic stem-cell transplant

ASV: Amplicon Sequence Variant

CI: Confidence interval

DOT: Days of therapy

DRI: Disease Risk Index

E: Engraftment

E30: 30 days after engraftment

E75: 75 days after engraftment

E. faecium: Enterococcus faecium

GCF: Gingival crevicular fluid

HR: Hazard ratio

LOT: Length of therapy

OM: Oral mucosa

OR: Odds ratio

OS: Overall survival

P: Preconditioning

PFS: Progression-free survival

SB: Supragingival biofilm

S. maltophilia: Stenotrophomonas maltophilia

SRS: Scaling with ranked subsampling

References

1. Welch JLM, Ramírez-Puebla ST, Borisy GG. Oral Microbiome Geography: Micron-Scale Habitat and Niche. Cell Host Microbe. 2020;28:160–8.

2. Rosier BT, Marsh PD, Mira A. Resilience of the Oral Microbiota in Health: Mechanisms That Prevent Dysbiosis. J Dent Res. 2018;97:371–80.

3. Proctor DM, Relman DA. The Landscape Ecology and Microbiota of the Human Nose, Mouth, and Throat. Cell Host Microbe. 2017;21:421–32.

4. Segata N, Haake SK, Mannon P, Lemon KP, Waldron L, Gevers D, et al. Composition of the adult digestive tract bacterial microbiome based on seven mouth surfaces, tonsils, throat and stool samples. Genome Biol. 2012;13:R42.

5. Tuganbaev T, Yoshida K, Honda K. The effects of oral microbiota on health. Science. 2022;376:934–6.

6. Takahashi N, Nyvad B. The Role of Bacteria in the Caries Process: Ecological Perspectives. J Dent Res. 2011;90:294–303.

7. Ng E, Tay JRH, Balan P, Ong MMA, Bostanci N, Belibasakis GN, et al. Metagenomic sequencing provides new insights into the subgingival bacteriome and aetiopathology of periodontitis. J Periodontal Res. 2021;56:205–18.

8. Gaffen SL, Moutsopoulos NM. Regulation of host-microbe interactions at oral mucosal barriers by type 17 immunity. Sci Immunol. 2020;5:eaau4594.

9. Dominy SS, Lynch C, Ermini F, Benedyk M, Marczyk A, Konradi A, et al. Porphyromonas gingivalis in Alzheimer's disease brains: Evidence for disease causation and treatment with small-molecule inhibitors. Sci Adv. 2019;5:eaau3333.

10. Snowden JA, Sánchez-Ortega I, Corbacioglu S, Basak GW, Chabannon C, de la

695 Camara R, et al. Indications for haematopoietic cell transplantation for haematological
696 diseases, solid tumours and immune disorders: current practice in Europe, 2022. Bone
697 Marrow Transplant. 2022;57:1217–39.

698 11. Jenq RR, van den Brink MRM. Allogeneic haematopoietic stem cell transplantation:
699 individualized stem cell and immune therapy of cancer. Nat Rev Cancer. 2010;10:213–21.

700 12. Gyurkocza B, Sandmaier BM. Conditioning regimens for hematopoietic cell
701 transplantation: one size does not fit all. Blood. 2014;124:344–53.

702 13. Welniak LA, Blazar BR, Murphy WJ. Immunobiology of Allogeneic Hematopoietic Stem
703 Cell Transplantation. Annu Rev Immunol. 2007;25:139–70.

704 14. Lehrnbecher T, Fisher BT, Phillips B, Alexander S, Ammann RA, Beauchemin M, et al.
705 Guideline for Antibacterial Prophylaxis Administration in Pediatric Cancer and Hematopoietic
706 Stem Cell Transplantation. Clin Infect Dis. 2020;71:226–36.

707 15. Schluter J, Peled JU, Taylor BP, Markey KA, Smith M, Taur Y, et al. The gut microbiota
708 is associated with immune cell dynamics in humans. Nature. 2020;588:303–7.

709 16. Zheng D, Liwinski T, Elinav E. Interaction between microbiota and immunity in health
710 and disease. Cell Res. 2020;30:492–506.

711 17. Ervin SM, Ramanan SV, Bhatt AP. Relationship Between the Gut Microbiome and
712 Systemic Chemotherapy. Dig Dis Sci. 2020;65:874–84.

713 18. Wang L, Wang X, Zhang G, Ma Y, Zhang Q, Li Z, et al. The impact of pelvic radiotherapy
714 on the gut microbiome and its role in radiation-induced diarrhoea: a systematic review.
715 Radiat Oncol Lond Engl. 2021;16:187.

716 19. Ramirez J, Guarner F, Bustos Fernandez L, Maruy A, Sdepanian VL, Cohen H.
717 Antibiotics as Major Disruptors of Gut Microbiota. Front Cell Infect Microbiol. 2020;10.

718 20. Shono Y, van den Brink MRM. Gut microbiota injury in allogeneic haematopoietic stem
719 cell transplantation. Nat Rev Cancer. 2018;18:283–95.

720 21. Sen T, Thummer RP. The Impact of Human Microbiotas in Hematopoietic Stem Cell and
721 Organ Transplantation. Front Immunol. 2022;13.

722 22. Ames NJ, Barb JJ, Ranucci A, Kim H, Mudra SE, Cashion AK, et al. The oral microbiome
723 of patients undergoing treatment for severe aplastic anemia: a pilot study. Ann Hematol.
724 2019;98:1351–65.

725 23. Shouval R, Eshel A, Dubovski B, Kuperman AA, Danylesko I, Fein JA, et al. Patterns of
726 salivary microbiota injury and oral mucositis in recipients of allogeneic hematopoietic stem
727 cell transplantation. Blood Adv. 2020;4:2912–7.

728 24. Heidrich V, Bruno JS, Knebel FH, de Molla VC, Miranda-Silva W, Asprino PF, et al.
729 Dental Biofilm Microbiota Dysbiosis Is Associated With the Risk of Acute Graft-Versus-Host
730 Disease After Allogeneic Hematopoietic Stem Cell Transplantation. Front Immunol. 2021;12.

731 25. de Molla VC, Heidrich V, Bruno JS, Knebel FH, Miranda-Silva W, Asprino PF, et al.
732 Disruption of the oral microbiota is associated with a higher risk of relapse after allogeneic
733 hematopoietic stem cell transplantation. Sci Rep. 2021;11:17552.

734 26. Laheij AMGA, Rozema FR, Brennan MT, von Bültzingslöwen I, van Leeuwen SJM,
735 Potting C, et al. Long-Term Analysis of Resilience of the Oral Microbiome in Allogeneic Stem
736 Cell Transplant Recipients. Microorganisms. 2022;10:734.

27. Liu C, Frank DN, Horch M, Chau S, Ir D, Horch EA, et al. Associations between acute gastrointestinal GvHD and the baseline gut microbiota of allogeneic hematopoietic stem cell transplant recipients and donors. Bone Marrow Transplant. 2017;52:1643–50.

28. Stein-Thoeringer CK, Nichols KB, Lazrak A, Docampo MD, Slingerland AE, Slingerland JB, et al. Lactose drives Enterococcus expansion to promote graft-versus-host disease. Science. 2019;366:1143–9.

29. Peled JU, Gomes ALC, Devlin SM, Littmann ER, Taur Y, Sung AD, et al. Microbiota as Predictor of Mortality in Allogeneic Hematopoietic-Cell Transplantation. N Engl J Med. 2020;382:822–34.

30. Oku S, Takeshita T, Futatsuki T, Kageyama S, Asakawa M, Mori Y, et al. Disrupted tongue microbiota and detection of nonindigenous bacteria on the day of allogeneic hematopoietic stem cell transplantation. PLOS Pathog. 2020;16:e1008348.

31. Stanić Benić M, Milanič R, Monnier AA, Gyssens IC, Adriaenssens N, Versporten A, et al. Metrics for quantifying antibiotic use in the hospital setting: results from a systematic review and international multidisciplinary consensus procedure. J Antimicrob Chemother. 2018;73 suppl_6:vi50–8.

32. Wang H, Altemus J, Niazi F, Green H, Calhoun BC, Sturgis C, et al. Breast tissue, oral and urinary microbiomes in breast cancer. Oncotarget. 2017;8:88122–38.

33. Klindworth A, Pruesse E, Schweer T, Peplies J, Quast C, Horn M, et al. Evaluation of general 16S ribosomal RNA gene PCR primers for classical and next-generation sequencing-based diversity studies. Nucleic Acids Res. 2013;41:e1.

34. Heng Li. seqtk: Toolkit for processing sequences in FASTA/Q formats.

35. Bolyen E, Rideout JR, Dillon MR, Bokulich NA, Abnet CC, Al-Ghalith GA, et al. Reproducible, interactive, scalable and extensible microbiome data science using QIIME 2. Nat Biotechnol. 2019;37:852–7.

36. Callahan BJ, McMurdie PJ, Rosen MJ, Han AW, Johnson AJA, Holmes SP. DADA2: High-resolution sample inference from Illumina amplicon data. Nat Methods. 2016;13:581–3.

37. Rognes T, Flouri T, Nichols B, Quince C, Mahé F. VSEARCH: a versatile open source tool for metagenomics. PeerJ. 2016;4:e2584.

38. Quast C, Pruesse E, Yilmaz P, Gerken J, Schweer T, Yarza P, et al. The SILVA ribosomal RNA gene database project: improved data processing and web-based tools. Nucleic Acids Res. 2013;41:D590–6.

39. R Core Team. R: A language and environment for statistical computing. R Found Stat Comput Vienna Austria. 2021.

40. Jordan E. Bisanz. qiime2R: Importing QIIME2 artifacts and associated data into R sessions. 2018.

41. Beule L, Karlovsky P. Improved normalization of species count data in ecology by scaling with ranked subsampling (SRS): application to microbial communities. PeerJ. 2020;8:e9593.

42. Simpson EH. Measurement of Diversity. Nature. 1949;163:688–688.

43. McMurdie PJ, Holmes S. phyloseq: An R Package for Reproducible Interactive Analysis and Graphics of Microbiome Census Data. PLOS ONE. 2013;8:e61217.

779 44. Orwin KH, Wardle DA. New indices for quantifying the resistance and resilience of soil
780 biota to exogenous disturbances. Soil Biol Biochem. 2004;36:1907–12.

781 45. Shade A, Peter H, Allison S, Baho D, Berga M, Buergmann H, et al. Fundamentals of
782 Microbial Community Resistance and Resilience. Front Microbiol. 2012;3.

783 46. Lozupone C, Lladser ME, Knights D, Stombaugh J, Knight R. UniFrac: an effective
784 distance metric for microbial community comparison. ISME J. 2011;5:169–72.

785 47. Daniel P. Smith. rbiom: Read/Write, Transform, and Summarize “BIOM” Data. 2022.

786 48. Lin H, Peddada SD. Analysis of compositions of microbiomes with bias correction. Nat
787 Commun. 2020;11:3514.

788 49. Cox DR. Regression Models and Life-Tables. J R Stat Soc Ser B Methodol.
789 1972;34:187–202.

790 50. Fine JP, Gray RJ. A Proportional Hazards Model for the Subdistribution of a Competing
791 Risk. J Am Stat Assoc. 1999;94:496–509.

792 51. Heidrich V, Karlovsky P, Beule L. ‘SRS’ R Package and ‘q2-srs’ QIIME 2 Plugin:
793 Normalization of Microbiome Data Using Scaling with Ranked Subsampling (SRS). Appl Sci.
794 2021;11:11473.

795 52. Kolenbrander PE, Palmer RJ, Periasamy S, Jakubovics NS. Oral multispecies biofilm
796 development and the key role of cell–cell distance. Nat Rev Microbiol. 2010;8:471–80.

797 53. Barrak I, Stájer A, Gajdács M, Urbán E. Small, but smelly: the importance of
798 Solobacterium moorei in halitosis and other human infections. Heliyon. 2020;6:e05371.

799 54. Komiyama EY, Lepesqueur LSS, Yassuda CG, Samaranayake LP, Parahitiyawa NB,
800 Balducci I, et al. Enterococcus Species in the Oral Cavity: Prevalence, Virulence Factors and
801 Antimicrobial Susceptibility. PLOS ONE. 2016;11:e0163001.

802 55. Caufield PW, Schön CN, Saraithong P, Li Y, Argimón S. Oral Lactobacilli and Dental
803 Caries: A Model for Niche Adaptation in Humans. J Dent Res. 2015;94 9_suppl:110S-118S.

804 56. Dong J, Li W, Wang Q, Chen J, Zu Y, Zhou X, et al. Relationships Between Oral
805 Microecosystem and Respiratory Diseases. Front Mol Biosci. 2022;8.

806 57. Gudiol C, Sabé N, Carratalà J. Is hospital-acquired pneumonia different in transplant
807 recipients? Clin Microbiol Infect. 2019;25:1186–94.

808 58. Taur Y, Xavier JB, Lipuma L, Ubeda C, Goldberg J, Gobourne A, et al. Intestinal
809 Domination and the Risk of Bacteremia in Patients Undergoing Allogeneic Hematopoietic
810 Stem Cell Transplantation. Clin Infect Dis. 2012;55:905–14.

811 59. Mark Welch JL, Dewhirst FE, Borisy GG. Biogeography of the Oral Microbiome: The
812 Site-Specialist Hypothesis. Annu Rev Microbiol. 2019;73:335–58.

813 60. Zaneveld JR, McMinds R, Vega Thurber R. Stress and stability: applying the Anna
814 Karenina principle to animal microbiomes. Nat Microbiol. 2017;2:1–8.

815 61. Cookson BD, Macrae MB, Barrett SP, Brown DFJ, Chadwick C, French GL, et al.
816 Guidelines for the control of glycopeptide-resistant enterococci in hospitals. J Hosp Infect.
817 2006;62:6–21.

818 62. Sahin U, Toprak SK, Atilla PA, Atilla E, Demirer T. An overview of infectious
819 complications after allogeneic hematopoietic stem cell transplantation. J Infect Chemother.
820 2016;22:505–14.

821 63. Thänert R, Reske KA, Hink T, Wallace MA, Wang B, Schwartz DJ, et al. Comparative
822 Genomics of Antibiotic-Resistant Uropathogens Implicates Three Routes for Recurrence of
823 Urinary Tract Infections. mBio. 2019;10:e01977-19.

824 64. Abed J, Maalouf N, Manson AL, Earl AM, Parhi L, Emgård JEM, et al. Colon Cancer-
825 Associated Fusobacterium nucleatum May Originate From the Oral Cavity and Reach Colon
826 Tumors via the Circulatory System. Front Cell Infect Microbiol. 2020;10.

827 65. Scheich S, Koenig R, Wilke AC, Lindner S, Reinheimer C, Wichelhaus TA, et al.
828 Stenotrophomonas maltophilia colonization during allogeneic hematopoietic stem cell
829 transplantation is associated with impaired survival. PLOS ONE. 2018;13:e0201169.

830 66. Li F, Wang Y, Sun L, Wang X. Vancomycin-resistant Enterococcus faecium pneumonia
831 in a uremic patient on hemodialysis: a case report and review of the literature. BMC Infect
832 Dis. 2020;20:167.

833 67. Dethlefsen L, Relman DA. Incomplete recovery and individualized responses of the
834 human distal gut microbiota to repeated antibiotic perturbation. Proc Natl Acad Sci. 2011;108
835 supplement_1:4554–61.

836 68. Vaitkute G, Panic G, Alber DG, Faizura-Yeop I, Cloutman-Green E, Swann J, et al.
837 Linking gastrointestinal microbiota and metabolome dynamics to clinical outcomes in
838 paediatric haematopoietic stem cell transplantation. Microbiome. 2022;10:89.

839 69. Zaura E, Brandt BW, Teixeira de Mattos MJ, Buijs MJ, Caspers MPM, Rashid M-U, et al.
840 Same Exposure but Two Radically Different Responses to Antibiotics: Resilience of the
841 Salivary Microbiome versus Long-Term Microbial Shifts in Feces. mBio. 2015;6:e01693-15.

842 70. Chng KR, Ghosh TS, Tan YH, Nandi T, Lee IR, Ng AHQ, et al. Metagenome-wide
843 association analysis identifies microbial determinants of post-antibiotic ecological recovery in
844 the gut. Nat Ecol Evol. 2020;4:1256–67.

845 71. Sommer F, Anderson JM, Bharti R, Raes J, Rosenstiel P. The resilience of the intestinal
846 microbiota influences health and disease. Nat Rev Microbiol. 2017;15:630–8.

847 72. Hooper LV, Littman DR, Macpherson AJ. Interactions Between the Microbiota and the
848 Immune System. Science. 2012;336:1268–73.

849 73. Martino C, Dilmore AH, Burcham ZM, Metcalf JL, Jeste D, Knight R. Microbiota
850 succession throughout life from the cradle to the grave. Nat Rev Microbiol. 2022;20:707–20.

851 74. Ng KM, Aranda-Díaz A, Tropini C, Frankel MR, Treuren WV, O'Loughlin CT, et al.
852 Recovery of the Gut Microbiota after Antibiotics Depends on Host Diet, Community Context,
853 and Environmental Reservoirs. Cell Host Microbe. 2019;26:650-665.e4.

854 75. Fiorenza S, Turtle CJ. Associations between the Gut Microbiota, Immune Reconstitution,
855 and Outcomes of Allogeneic Hematopoietic Stem Cell Transplantation. Immunometabolism.
856 2021;3:e210004.

857 76. Ingham AC, Kielsen K, Cilieborg MS, Lund O, Holmes S, Aarestrup FM, et al. Specific
858 gut microbiome members are associated with distinct immune markers in pediatric
859 allogeneic hematopoietic stem cell transplantation. Microbiome. 2019;7:131.

860 77. Miltiadous O, Waters NR, Andrlová H, Dai A, Nguyen CL, Burgos da Silva M, et al. Early
861 intestinal microbial features are associated with CD4 T-cell recovery after allogeneic
862 hematopoietic transplant. Blood. 2022;139:2758–69.

863 78. Staffas A, Silva MB da, Slingerland AE, Lazrak A, Bare CJ, Holman CD, et al. Nutritional

Support from the Intestinal Microbiota Improves Hematopoietic Reconstitution after Bone Marrow Transplantation in Mice. Cell Host Microbe. 2018;23:447-457.e4.

79. Nath S, Zilm P, Jamieson L, Kapellas K, Goswami N, Ketagoda K, et al. Development and characterization of an oral microbiome transplant among Australians for the treatment of dental caries and periodontal disease: A study protocol. PLOS ONE. 2021;16:e0260433.

80. Abdill RJ, Adamowicz EM, Blekhman R. Public human microbiome data are dominated by highly developed countries. PLOS Biol. 2022;20:e3001536.

81. Jin S, Wetzel D, Schirmer M. Deciphering mechanisms and implications of bacterial translocation in human health and disease. Curr Opin Microbiol. 2022;67:102147.

Acknowledgements

Not applicable.

Funding

VH was supported by Fundação de Amparo à Pesquisa do Estado de São Paulo (FAPESP, process no. 13996-0/2018). FHK was supported by FAPESP (process no. 16854-4/2015).

Author information

Authors and Affiliations

Centro de Oncologia Molecular, Hospital Sírio-Libanês, São Paulo, SP, Brazil

Vitor Heidrich, Franciele H. Knebel, Julia S. Bruno, Wanessa Miranda-Silva, Paula F. Asprino, Eduardo R. Fregnani, Anamaria A. Camargo

Departamento de Bioquímica, Instituto de Química, Universidade de São Paulo, São Paulo, SP, Brazil

Vitor Heidrich

Centro de Oncologia, Hospital Sírio-Libanês, São Paulo, SP, Brazil

Luciana Tucunduva, Yana Novis

Hospital Nove de Julho, Rede DASA, São Paulo, SP, Brazil

Vinícius C. de Molla, Celso Arrais-Rodrigues

Universidade Federal de São Paulo, São Paulo, SP, Brazil

31

Vinícius C. de Molla, Celso Arrais-Rodrigues

Hospital das Clínicas da Faculdade de Medicina, Universidade de São Paulo/Instituto do Câncer do Estado de São Paulo (ICESP), São Paulo, SP, Brazil

Vanderson Rocha

Contributions

EFR and AAC designed the study. VCM, LT, VR, YN, and CAR recruited and clinically evaluated volunteers. VCM collected data from clinical records. WMS collected oral samples. FHK processed most of the samples. FHK and PFA performed the sequencing. VH and AC conceptualized the analysis. VH performed all bioinformatics and statistical analyses. VH, JSB, and AAC contributed to the interpretation of results. VH and AAC wrote the original draft of the manuscript. VH, JSB, VCM, PFA, CAR, and AAC reviewed and edited the manuscript. All authors read and approved the final manuscript.

Corresponding author

Correspondence to Anamaria A. Camargo.

Ethics declarations

Ethics approval and consent to participate

This study was approved by the Ethics Committee of Hospital Sírio-Libanês (#HSL 2016-08), in line with the Declaration of Helsinki. All patients provided their written informed consent to participate.

Consent for publication

Not applicable.

Competing interests

The authors declare that they have no competing interests.

Figure legends

Figure 1

a Principal Coordinate Analysis (PCoA) of microbiota distances (weighted UniFrac) between oral sites for each timepoint. Ellipsoids indicate 95% confidence intervals. **b** Magnitude (PERMANOVA F) of distances (weighted UniFrac) between oral sites per timepoint. **c** Minimum distance (weighted UniFrac) between oral sites within patients per timepoint. Mann-Whitney U test was used with preconditioning (P) as the reference for comparisons. **d** Number of differentially abundant genera (ANCOM-BC) between oral sites per timepoint. GCF, gingival crevicular fluid; OM, oral mucosa; SB, supragingival biofilm; A, aplasia; E, engraftment; E30, 30 days after engraftment; E75, 75 days after engraftment; **, P-value < 0.01; ***, P-value < 0.001.

Figure 2

a Diversity (Gini-Simpson) per timepoint for each oral site. Mann-Whitney U test was used with preconditioning (P) as the reference for comparisons. **b** Diversity resistance, resilience, and stability (see Methods) per oral site. Mann-Whitney U test was used. Distance to P centroid (weighted UniFrac) per timepoint for each oral site. Mann-Whitney U test was used with P as the reference for comparisons. **d** Magnitude (PERMANOVA F) of distances (weighted UniFrac) between P and other timepoints for each site. GCF, gingival crevicular fluid; OM, oral mucosa; SB, supragingival biofilm; A, aplasia; E, engraftment; E30, 30 days after engraftment; E75, 75 days after engraftment; *, P-value < 0.05; **, P-value < 0.01; ***, P-value < 0.001; ****, P-value < 0.0001.

Figure 3

a Mean genera relative abundances (RA) per timepoint for each oral site. Genera with >2% mean RA in any combination of oral site and timepoint are shown. **b** Mean genera RA ranking per timepoint for each oral site. Top-10 genera are shown. **c** Differentially abundant genera (ANCOM-BC) between P and other timepoints for each site. GCF, gingival crevicular fluid; OM, oral mucosa; SB, supragingival biofilm; P, preconditioning; A, aplasia; E, engraftment; E30, 30 days after engraftment; E75, 75 days

33

after engraftment; *, q-value < 0.05; **, q-value < 0.01; ***, q-value < 0.001; z, ANCOM-BC structural zero.

Figure 4

a-c Proportion of blooming events per oral site (a), timepoint (b) and genus (c). **d** Number of blooming events per genus in each oral site. GCF, gingival crevicular fluid; OM, oral mucosa; SB, supragingival biofilm; A, aplasia; E, engraftment; E30, 30 days after engraftment; E75, 75 days after engraftment.

Figure 5

a Antibiotic agents used by each patient between preconditioning (P) and 30 days after engraftment (E30). **b** Time of antibiotic administration (LOT: length of therapy; DOT: days of therapy) among patients showing and not showing blooms between P and E30. **c** Patient #2: genera relative abundance dynamics for each oral site (top) and antibiotic usage timeline (bottom). Genera with >1% mean relative abundance in any combination of oral site and timepoint are shown. GCF, gingival crevicular fluid; OM, oral mucosa; SB, supragingival biofilm; A, aplasia; E, engraftment; E75, 75 days after engraftment; SC, stem-cell; vanc, vancomycin; tige, tigecycline; tazo, piperacillin tazobactam; poli, polymyxin B; mero, meropenem; line, linezolid.

Figure 6

a Relationship between diversity resistance, resilience, and stability values calculated for each patient. **b** Extent of compositional shifts (weighted UniFrac) between consecutive timepoints (adjusted for the time in days between timepoints) for each oral site. The line indicates the median value per interval. **c** Distance (weighted UniFrac) to timepoint centroid per timepoint for each oral site. Mann-Whitney U test was used with preconditioning (P) as the reference for comparisons. **d** Pairwise distances (weighted UniFrac) per timepoint (all-against-all) for each oral site. Mann-Whitney U test was used with P as the reference for comparisons. **e** Distance to P (weighted UniFrac) at engraftment (E) and 30 days after engraftment (E30) for each patient for each oral site. The thick line indicates the median value at each timepoint. GCF, gingival crevicular fluid; OM, oral mucosa; SB, supragingival biofilm; A, aplasia; E75, 75 days after engraftment; **, P-value < 0.01; ***, P-value < 0.001; ****, P-value < 0.0001.

Figure 7

34

a Principal Coordinate Analysis (PCoA) with representative microbiota trajectories of an oral mucosa (OM) recoverer and non-recoverer. **b** Recovery classifications per site for each patient. Patient #1 OM recovery could not be evaluated due to missing samples. **c-d** Kaplan-Meier curves comparing overall survival (c) and progression-free survival (d) among OM recoverers (R) and non-recoverers (NR). **e** Cumulative incidence curves of relapse among OM R and OM NR. **f-h** multivariate analysis for overall survival (f), progression-free survival (g), and risk of relapse (h). Each model includes OM recovery and the clinical variables that are relevant for each outcome. P, preconditioning; A, aplasia; E, engraftment; E30, 30 days after engraftment; E75, 75 days after engraftment; HR, hazard ratio; DRI, disease risk index; DOT, days of antibiotic therapy; Cond Int, conditioning intensity.

Figure 8

a Diversity (Gini-Simpson) among oral mucosa (OM) recoverers and non-recoverers for each timepoint. Mann-Whitney U test was used. **b** Correlation between diversity (Gini-Simpson) at preconditioning (P) and the compositional distance (weighted UniFrac) between P and 30 days after engraftment (E30) for each oral site. Spearman's rank correlation test was used. **c** Blood cell counts among OM recoverers and non-recoverers per timepoint for each blood cell type. Red dotted horizontal lines indicate normal counts (within reference values). Mann-Whitney U test was used. A, aplasia; E, engraftment; E75, 75 days after engraftment; *, P-value < 0.05; **, P-value < 0.01.

Supplementary information

Additional file 1: Timelines of antibiotic usage.

Antibiotic usage timelines for each patient in relation to stem-cell infusion. Red dashed line indicates preconditioning sampling. Red solid line indicates stem-cell infusion. Blue solid line indicates stem-cell engraftment. Blue dashed line indicates 30 days after engraftment sampling. clav, amoxicillin clavulanate; tazo, piperacillin tazobactam; amox, amoxicillin; cefe, cefepime; mero, meropenem; metr, metronidazole; ceft, ceftriaxone; vanc, vancomycin; teic, teicoplanin; cipr, ciprofloxacin; levo, levofloxacin; doxi, doxycycline; ampi, ampicillin; clar, clarithromycin; bact, sulfamethoxazole trimethoprim; erta, ertapenem; poli, polymyxin b; dapt, daptomycin;line, linezolid; tige, tigecycline; amic, amikacin.

35

994 **Additional file 2: Supplementary tables and figures.**

995 Supplementary material with 9 tables and 14 figures.

996 **Additional file 3: Supplementary methods.**

997 Supplementary text to the Materials and methods section.

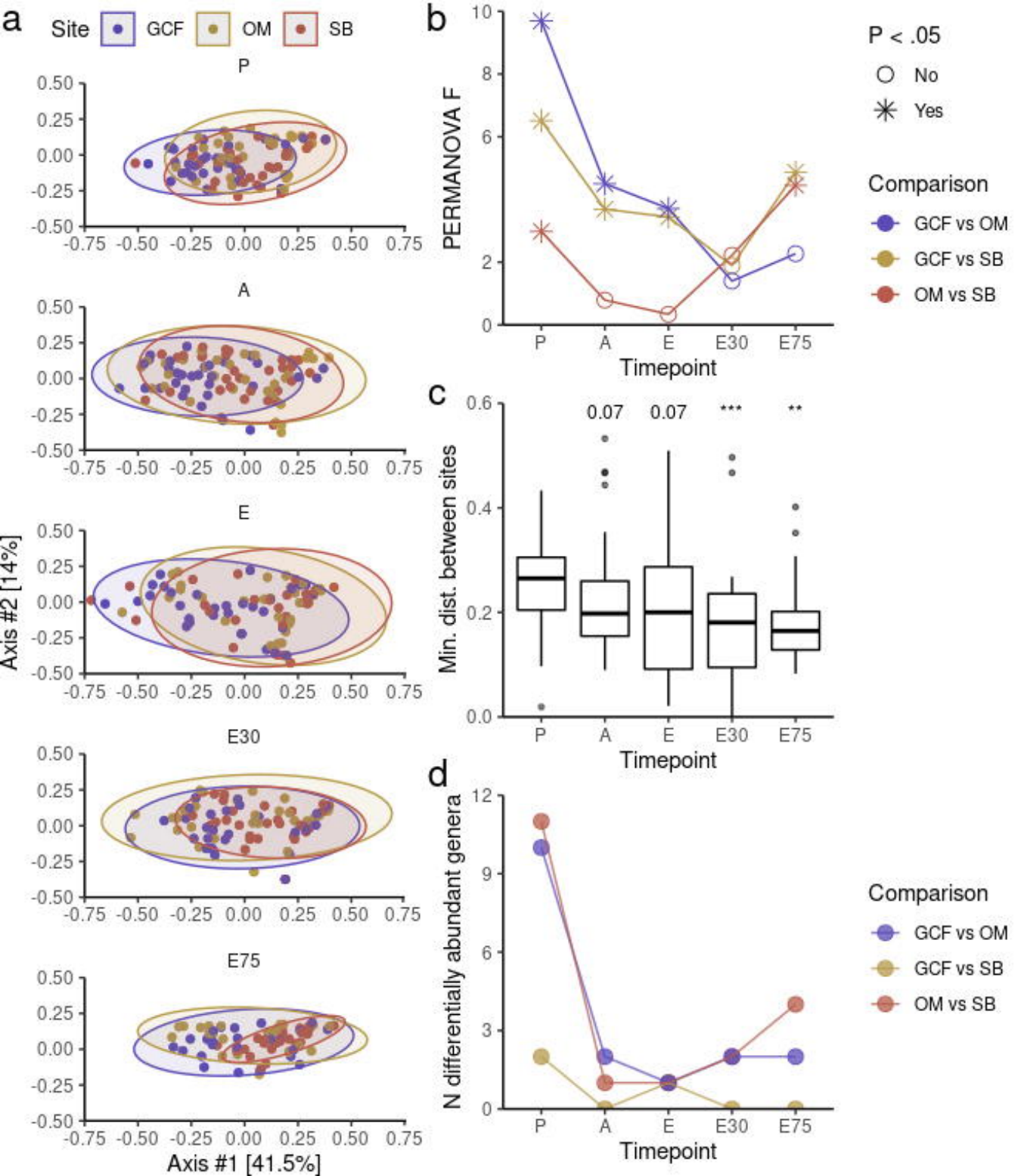
a
Site
GCF
OM
SB
P
A
E
E30
E75
Axis #2 [14%]
Axis #1 [41.5%]
b
PERMANOVA F
Timepoint
P < .05
No
Yes
Comparison
GCF vs OM
GCF vs SB
OM vs SB
c
Min. dist. between sites
0.07
0.07
***
**
Timepoint
d
N differentially abundant genera
Timepoint
Comparison
GCF vs OM
GCF vs SB
OM vs SB

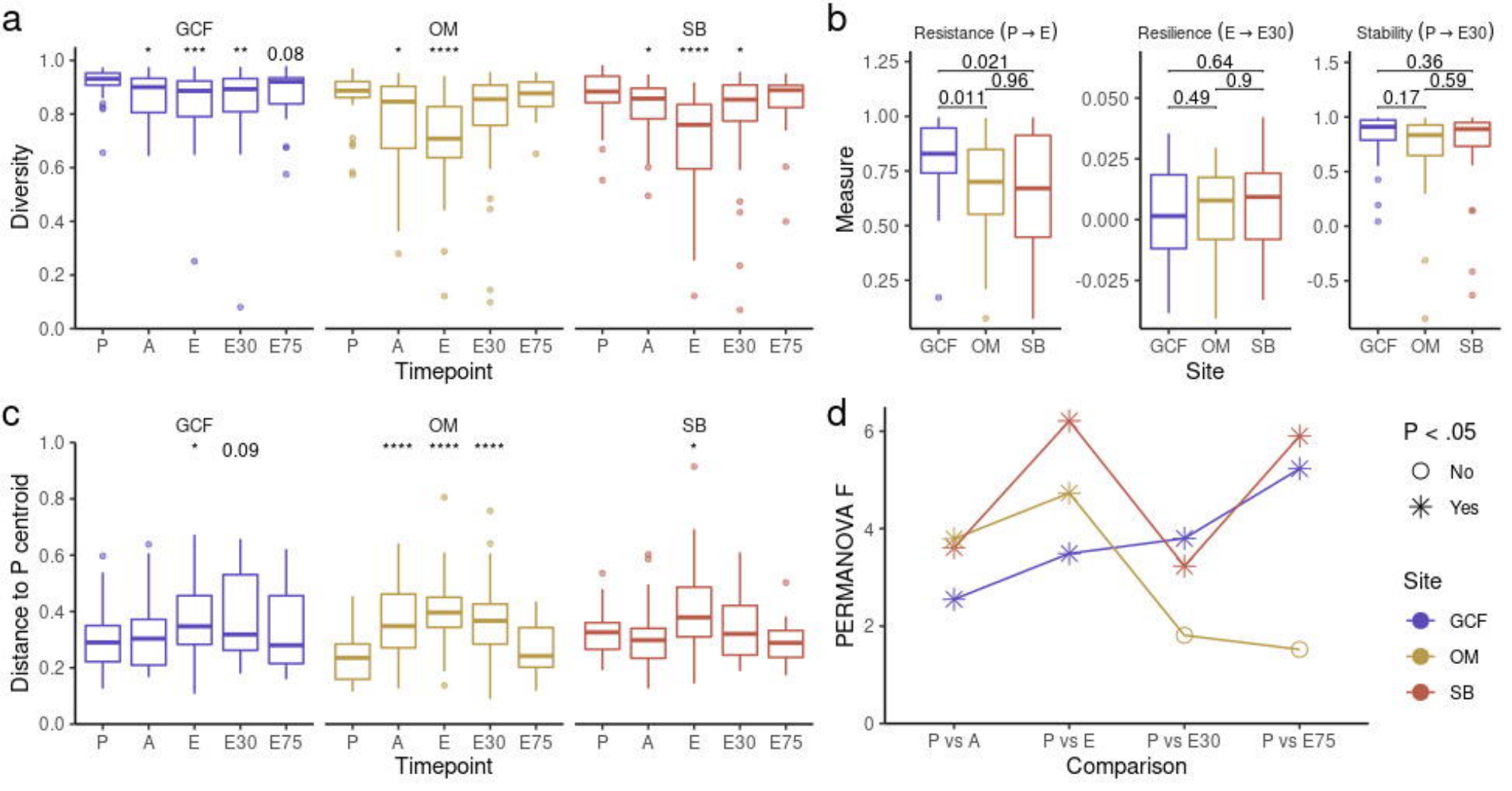
a
GCF
OM
SB
Diversity
Timepoint
P
A
E
E30
E75
0.08
b
Resistance (P → E)
Resilience (E → E30)
Stability (P → E30)
Measure
Site
GCF
OM
SB
0.021
0.96
0.011
0.64
0.9
0.49
0.36
0.59
0.17
c
Distance to P centroid
0.09
d
PERMANOVA F
Comparison
P vs A
P vs E
P vs E30
P vs E75
P < .05
No
Yes
Site

a

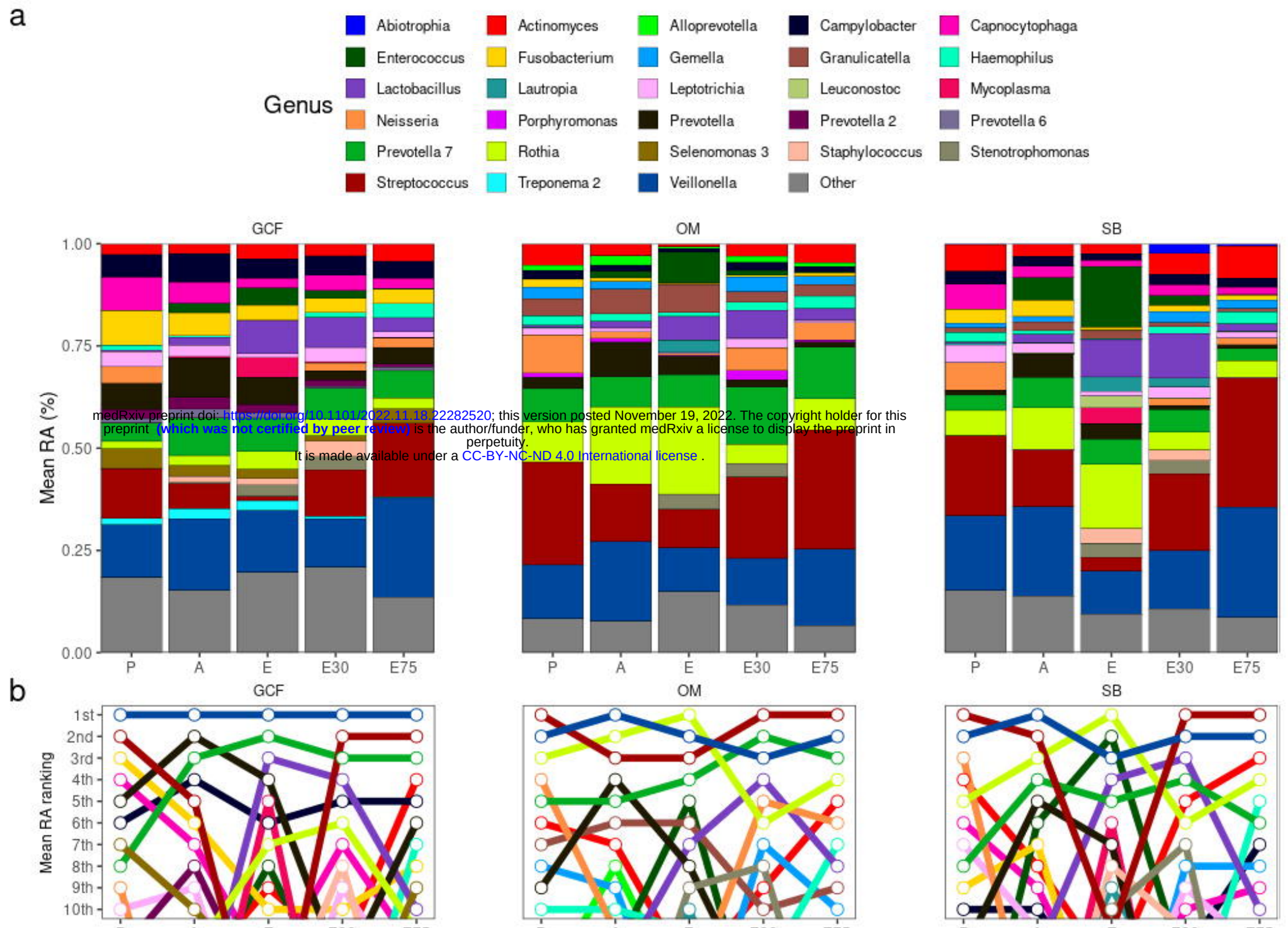

b

c

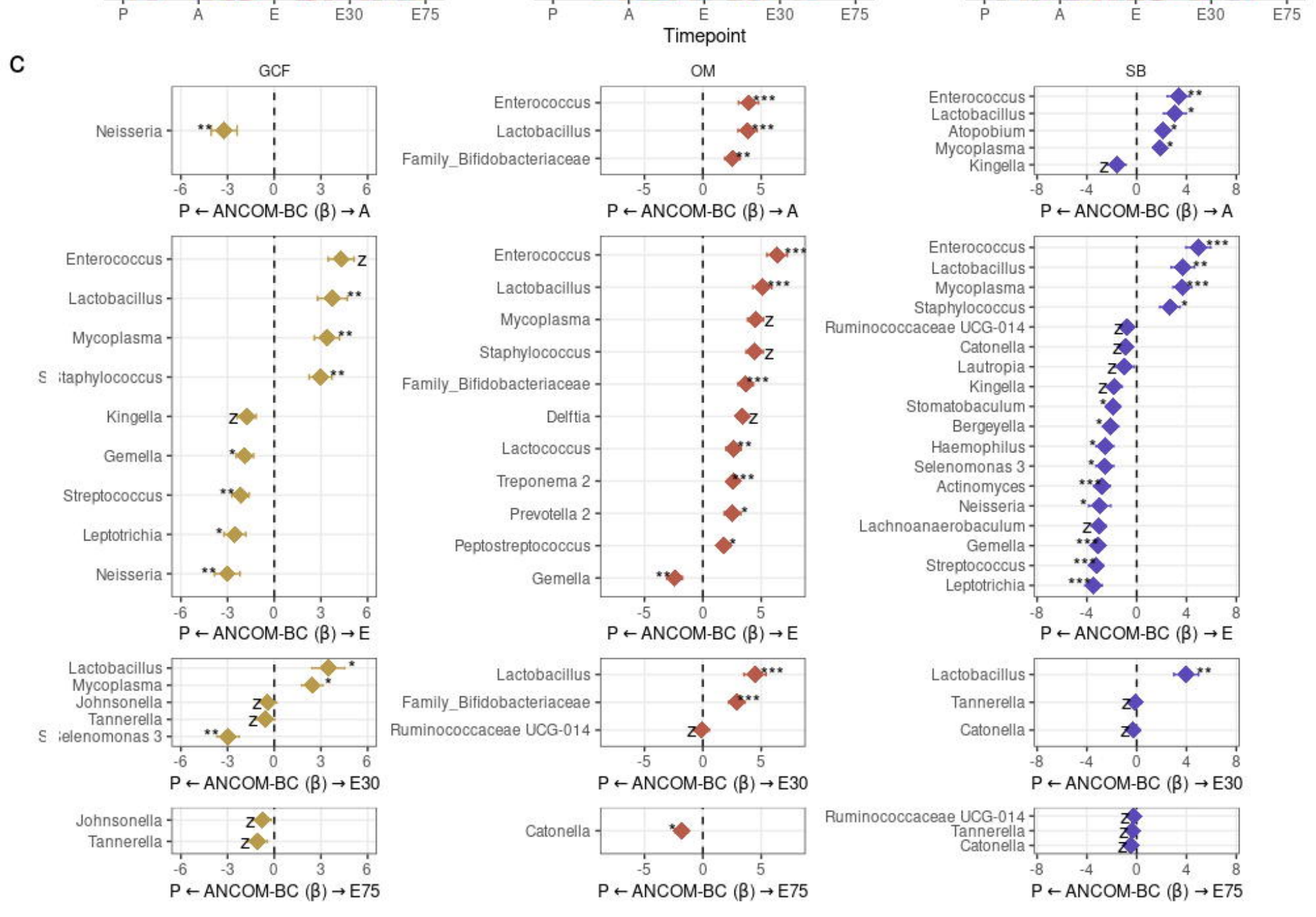

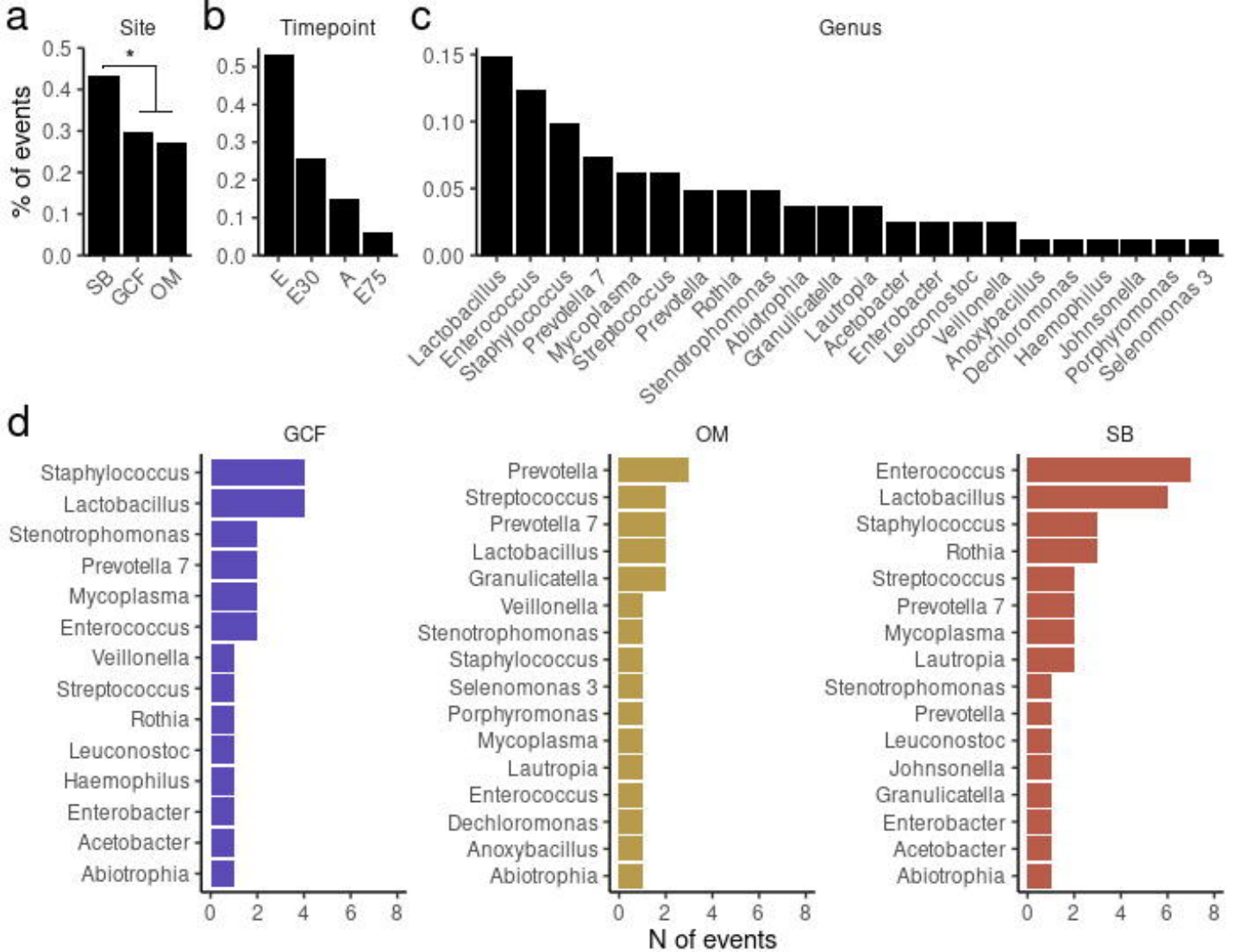
a
Site
% of events
0.5
0.4
0.3
0.2
0.1
0.0
*
SB
GCF
OM
b
Timepoint
0.5
0.4
0.3
0.2
0.1
0.0
E
E30
A
E75
c
Genus
0.15
0.10
0.05
0.00
Lactobacillus
Enterococcus
Staphylococcus
Prevotella 7
Mycoplasma
Streptococcus
Prevotella
Rothia
Stenotrophomonas
Abiotrophia
Granulicatella
Lautropia
Acetobacter
Enterobacter
Leuconostoc
Veillonella
Anoxybacillus
Dechloromonas
Haemophilus
Johnsonella
Porphyromonas
Selenomonas 3
d
GCF
Staphylococcus
Lactobacillus
Stenotrophomonas
Prevotella 7
Mycoplasma
Enterococcus
Veillonella
Streptococcus
Rothia
Leuconostoc
Haemophilus
Enterobacter
Acetobacter
Abiotrophia
0
2
4
6
8
OM
Prevotella
Streptococcus
Prevotella 7
Lactobacillus
Granulicatella
Veillonella
Stenotrophomonas
Staphylococcus
Selenomonas 3
Porphyromonas
Mycoplasma
Lautropia
Enterococcus
Dechloromonas
Anoxybacillus
Abiotrophia
0
2
4
6
8
N of events
SB
Enterococcus
Lactobacillus
Staphylococcus
Rothia
Streptococcus
Prevotella 7
Mycoplasma
Lautropia
Stenotrophomonas
Prevotella
Leuconostoc
Johnsonella
Granulicatella
Enterobacter
Acetobacter
Abiotrophia
0
2
4
6
8

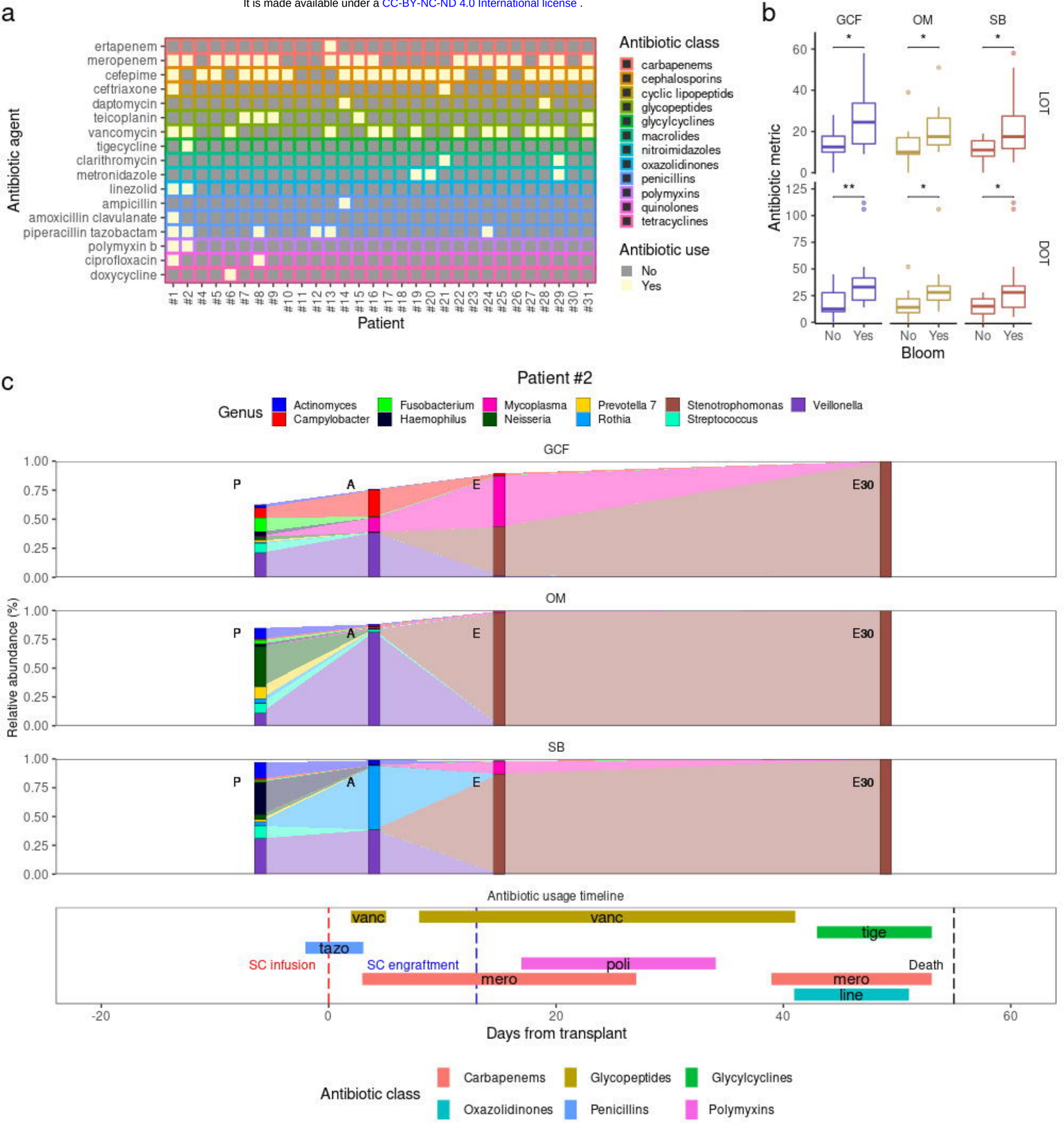

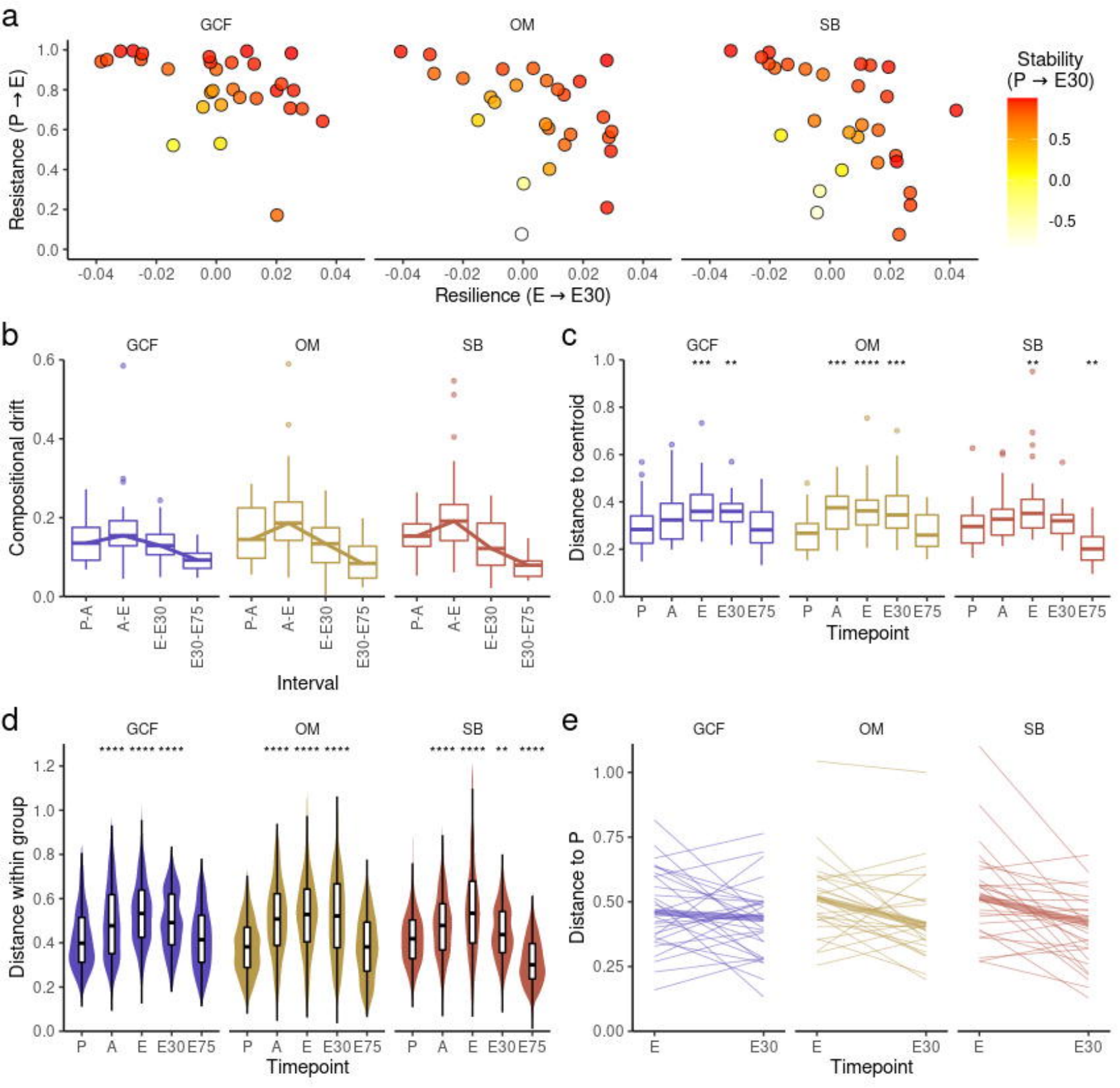
a
GCF
OM
SB
Resistance (P → E)
Resilience (E → E30)
Stability
(P → E30)
b
Compositional drift
Interval
P-A
A-E
E-E30
E30-E75
c
Distance to centroid
Timepoint
P
A
E
E30
E75
d
Distance within group
e
Distance to P

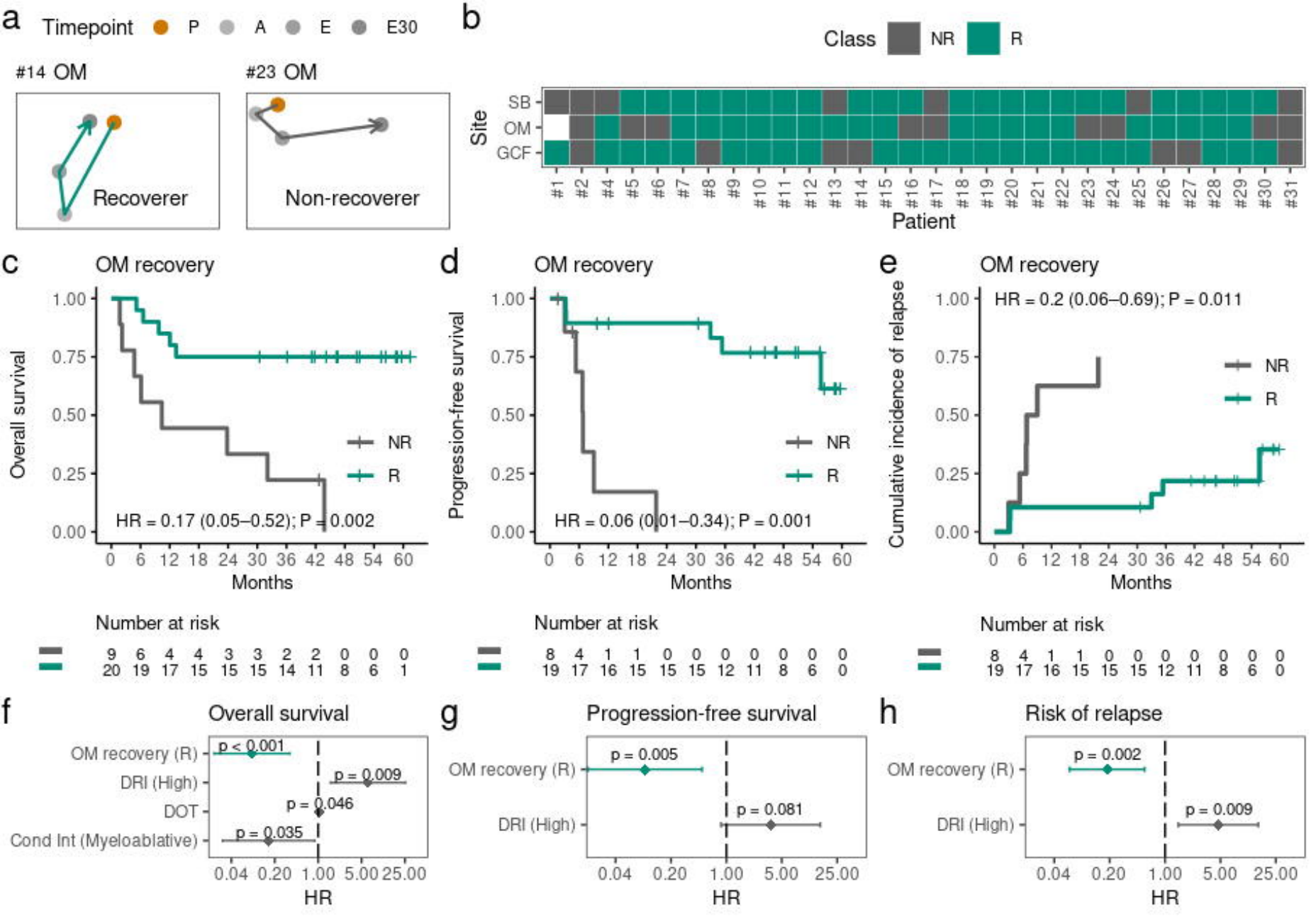
a
Timepoint
P
A
E
E30
#14 OM
#23 OM
Recoverer
Non-recoverer
b
Class
NR
R
Site
SB
OM
GCF
Patient
c
OM recovery
Overall survival
HR = 0.17 (0.05–0.52); P = 0.002
Months
Number at risk
d
OM recovery
Progression-free survival
HR = 0.06 (0.01–0.34); P = 0.001
Months
Number at risk
e
OM recovery
Cumulative incidence of relapse
HR = 0.2 (0.06–0.69); P = 0.011
Months
Number at risk
f
Overall survival
OM recovery (R)
DRI (High)
DOT
Cond Int (Myeloablative)
p < 0.001
p = 0.009
p = 0.046
p = 0.035
HR
g
Progression-free survival
OM recovery (R)
DRI (High)
p = 0.005
p = 0.081
HR
h
Risk of relapse
OM recovery (R)
DRI (High)
p = 0.002
p = 0.009
HR

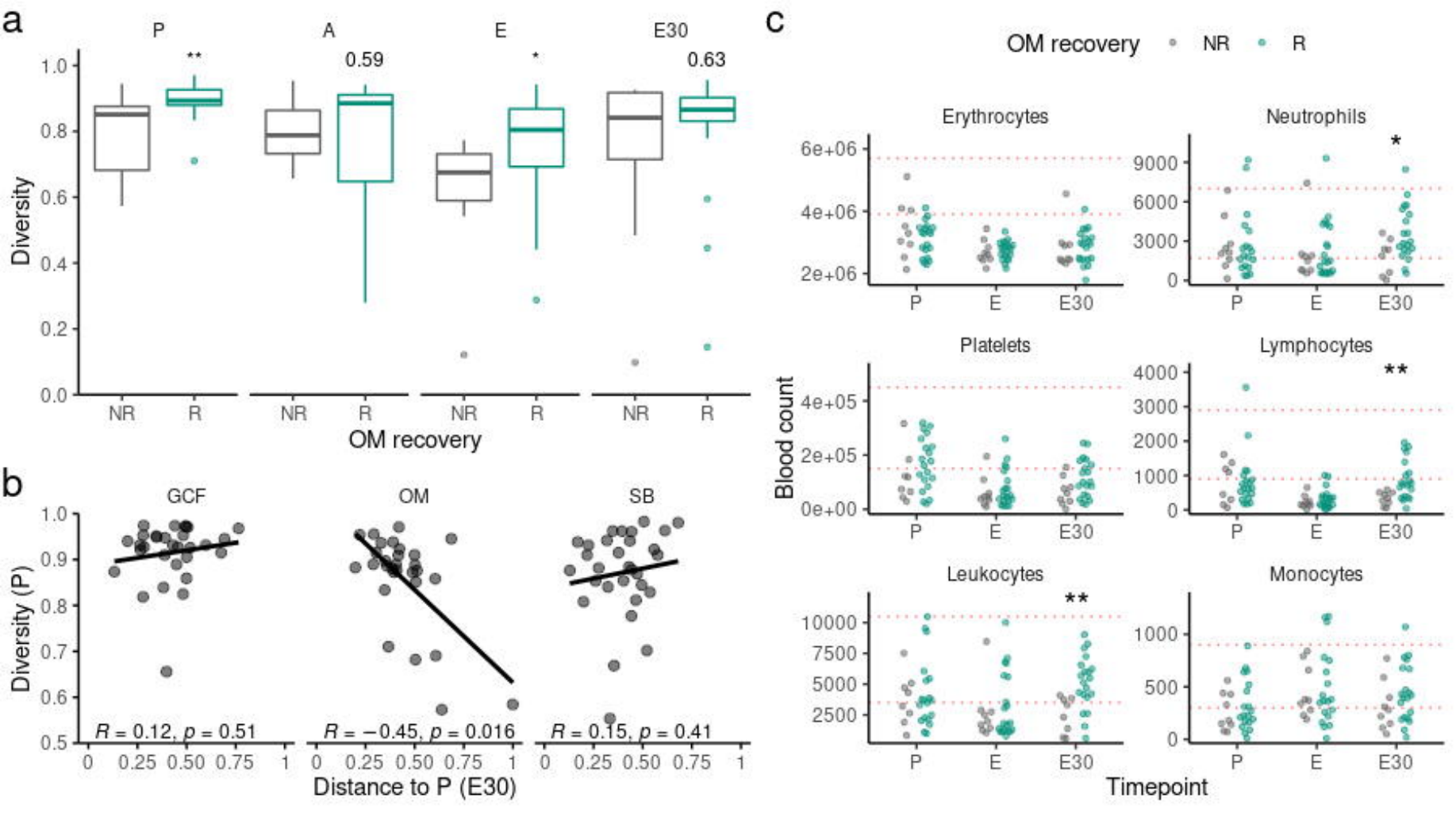
a
P
A
E
E30
**
0.59
*
0.63
Diversity
NR
R
OM recovery
b
GCF
OM
SB
Diversity (P)
R = 0.12, p = 0.51
R = −0.45, p = 0.016
R = 0.15, p = 0.41
Distance to P (E30)
c
OM recovery
NR
R
Erythrocytes
Neutrophils
Platelets
Lymphocytes
Leukocytes
Monocytes
Blood count
Timepoint